

1 ***Interactive Comment on “Tracing the origin of the oxygen-consuming organic***
2 ***matter in the hypoxic zone in a large eutrophic estuary: the lower reach of the***
3 ***Pearl River Estuary, China” by Su et al.***

4
5 Jianzhong Su¹, Minhan Dai^{1*}, Biyan He^{1, 2}, Lifang Wang¹, Jianping Gan³, Xianghui
6 Guo¹, Huade Zhao¹ and Fengling Yu¹

7 ¹State Key Laboratory of Marine Environmental Science, Xiamen University, Xiamen,
8 China

9 ²College of Food and Biological Engineering, Jimei University, Xiamen, China

10 ³Department of Mathematics and Division of Environment, Hong Kong University of
11 Science and Technology, Kowloon, Hong Kong, China

12 *Correspondence to: Minhan Dai (mdai@xmu.edu.cn)

13
14 Referee #1

15 Authors responded to all my original comments, but I feel that authors do not take into
16 account main points of my comments.

17 - Uncertainties and difference between the CJE and PRE (similar issue was raised by
18 reviewer #1): Authors re-estimated 13C value of organic carbon remineralized in the
19 hypoxic zone to be -23.2 +/- 1.1, which was originally -21.8 +/- 0.6. Such a large
20 change seems to be simply due to slight changes in end-member values. Authors may
21 have to allow seasonal and spatial variations of end-members. Indeed, the large
22 scattering and outlier evaluation in Figure 8 will result in much larger uncertainties in
23 13C value of OC remineralized. Authors should explain how the scattering and outlier
24 are included in the uncertainty (+/- 1.1) of OC remineralized values calculated. In
25 addition, I still do not see the visible difference between CJE and PRE in Figure 8
26 considering the scattering and natural variations. I think that authors try to obtain the
27 accuracy that the method cannot provide.

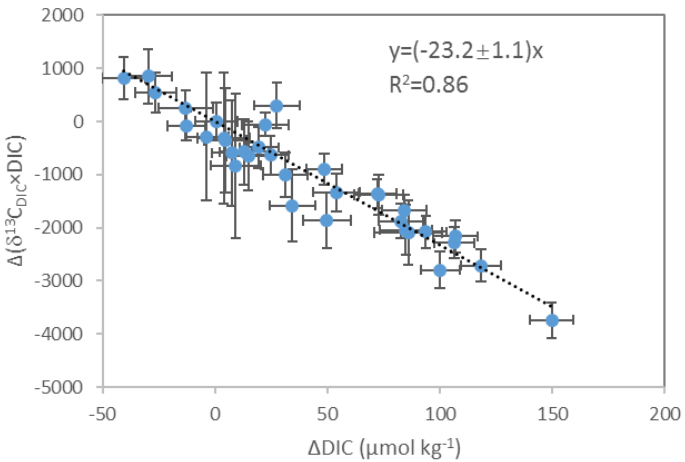
28 [Response]: We have to clarify that we did not change the end-member values of our
29 three end-member mixing model in either θ , S, DIC or $\delta^{13}\text{C}_{\text{DIC}}$. These end-member
30 values have been well justified by taking into account the uncertainties as explicitly
31 explained in our revised submission. The uncertainties of end-member values mostly
32 come from averaging values of several stations at certain salinity, thus including spatial
33 variations to some extent.

1 The reviewer might be right about the seasonality of the end-member values but here
2 we are examining the summer bottom hypoxia where the mixing scheme of the water
3 masses is rather clear as demonstrated in the T-S diagram shown in Fig. 7a.

4
5 A broader range of data at oxygen deficiency (n=38) (instead of those associated with
6 severe oxygen deficiency at $\text{AOU} > 100 \mu\text{mol kg}^{-1}$ (n=9) in our original submission) is
7 now being used to derive $\delta^{13}\text{C}_{\text{OCx}}$ considering on the main comments from Reviewer
8 #1. This re-estimation is justified because the oxygen depletion generating from
9 organic matter remineralization distributes as a continuum in the water column and the
10 accumulative oxygen reduction ultimately results in hypoxia formation.

11
12 As shown in Fig. 8, we plotted $\Delta(\delta^{13}\text{C}_{\text{DIC}} \times \text{DIC})$ against ΔDIC including all the
13 scattering points in the subsurface water in the PRE, and obtained a slope of $-23.2 \pm 1.1 \text{ ‰}$
14 with a high correlation coefficient ($R^2=0.86$, $P < 0.001$). Thus, the original $\delta^{13}\text{C}$
15 signature of the remineralized organic matter is -23.2 ‰ with an uncertainty of
16 $\pm 1.1 \text{ ‰}$.

17
18 The propagation error is shown in the following figure (Fig. S1). We are not sure how
19 the reviewer concluded that there was no visible difference between PRE and CJE.
20 The linear regression slope of the PRE is $-23.2 \pm 1.1 \text{ ‰}$, which is statistically different
21 from that of the CJE ($-18.5 \pm 1.0 \text{ ‰}$, $R^2=0.6$, $P < 0.001$). Our statistic has a confidence
22 level of 95 %.



23

24 Figure S1. Propagation errors for $\Delta(\delta^{13}\text{C}_{\text{DIC}} \times \text{DIC})$ and ΔDIC in Fig. 8.

1
2
3
4
5
6
7
8
9
10
11
12
13
14
15
16
17
18
19
20
21
22
23
24
25
26
27
28
29
30
31
32
33

- Use of Ca²⁺ as a conservative tracer: I am not convinced why authors use Ca, instead of salinity, as a conservative tracer although Ca is less conservative.

[Response]: We perfectly agreed that Ca²⁺ is a less conservative tracer than salinity. The fact is that salinity has been applied as a conservative tracer in our three end-member mixing model, and thus we ought to find alternative independent tracers to validate the model. Ca²⁺ is obviously such an alternative. As we explained in our previous responses, Ca²⁺ is conservative in our system as supported by a strong linear relationship between surface water Ca²⁺ and salinity, and aragonite oversaturation ($\Omega_{\text{arag}}=2.6\pm0.7$) in the subsurface water.

- Relative contribution of bottom sediment OM: Authors may compare the water column DO consumption rates relative to the bottom sediment DO consumption rates in order to show that the contribution of bottom sediments are negligible. Figure 4 shows stronger DO consumption in the bottom layer intuitively.

[Response]: In the present study, we used bottom water taken from Station A10 on 27 July and conducted on-deck incubation experiments to estimate total oxygen consumption rate, which was 9.8 $\mu\text{mol L}^{-1} \text{d}^{-1}$. Such a water column oxygen consumption rate could well support the oxygen decline rate observed in situ at Station A10 in the hypoxic zone between 20 July and 27 July (Fig. 6), which was 7.7 $\mu\text{mol L}^{-1} \text{d}^{-1}$. This first order comparison strongly suggests that water column oxygen consumption may be predominate in the formation of the hypoxia in the present case.

Note that we cannot distinguish between the contribution of resuspended sediments vs. sinking POC to oxygen depletion, because both of these isotopic signals would have been reflected in oxidation product (DIC) and the derived $\delta^{13}\text{C}$ value of the remineralized OC ($\delta^{13}\text{C}_{\text{OCx}}$). Please see details in our previous response to comment (3) of Referee #2. Quantifying the relative contribution of bottom sediment OM is beyond the scope of our present study. Moreover, the bottom sediment DO consumption rate is still controversial due to its high spatial variability.

In responding to the concerns of the reviewer, we have added in the further revised manuscript our water column total oxygen consumption rate determined by on-deck

1 incubation experiments using bottom water taken from Station A10 (Table S1). “As
 2 a first order comparison, the water column total oxygen consumption rate of 9.8 μmol
 3 $\text{L}^{-1} \text{d}^{-1}$ could well support the oxygen decline rate observed at Station A10 in the
 4 hypoxic zone between 20 July and 27 July (Fig. 6), which was 7.7 $\mu\text{mol L}^{-1} \text{d}^{-1}$. This
 5 comparison along with the stoichiometry between ΔDIC and AOU strongly suggests
 6 that water column aerobic respiration may be predominate in the formation of the
 7 hypoxia in the present case.” Please see P4 L14-20 and P10 L12-18 in the further
 8 revised manuscript.

9

10 Table S1. Comparison of oxygen consumption rate between in situ observations and
 11 on-deck incubation experiments at Stations A10 in the hypoxic zone.

Station	DO _{ini} ($\mu\text{mol L}^{-1}$)	DO _{end} ($\mu\text{mol L}^{-1}$)	Interval (d)	ΔDO ($\mu\text{mol L}^{-1}$)	DO decline rate ($\mu\text{mol L}^{-1} \text{d}^{-1}$)	Total oxygen consumption rate ($\mu\text{mol L}^{-1} \text{d}^{-1}$)
A10	156	101	7.1	55	7.7	9.8

12 Note that the subscripts “ini” means the initial sampling and “end” means the end
 13 sampling. The Interval shows the days between these two repeated sampling. DO
 14 decline rate equals to the amount of DO reduction dividing by interval.

15

16 - Significant figures: Authors show that DO and DIC precisions are +/- 1 and 2
 17 respectively. But, they say that “we kept one decimal place for DO/DIC...”. Authors
 18 should explain why they keep one decimal place although the values are meaningless.
 19 [Response]: Accepted. Do not keep one decimal place of DO/DIC in the main text.

20

21 Referee #2

22 The revisions made in the paper by Su et al. have substantially improved the quality of
 23 the paper which, to my opinion, is now ready for publication. You have answered the
 24 main points raised in my previous review, especially the one dealing with end-members
 25 which is crucial in quantifying the uncertainty of the message provided by the paper. I
 26 can see that you have changed the value and expanded the uncertainty of your
 27 proportion of terrigenous OM in the mix generating hypoxia.

28 I particularly appreciated the long and detailed response letter which made the revisions

1 easy to check and evaluate.

2 I have just a few technical points which should further improve the clarity of your
3 paper:

4 - You use very often "pre" for predicted (by the mixing model) and "PRE" for Pearl
5 River Estuary. It is confusing in the equations and Figures when endmembers are
6 quoted (Eq. 7 page 10, or Figure caption and axis labels of Figure 7). In this Figure (7)
7 especially, "PRE" and "pre" co-exist in the axis title which should be changed. You
8 should choose one of them (e.g. Pearl River Estuary) and replace "pre" by "mod" for
9 model.

10 [Response]: Accepted. Use “con” (conservative) instead of “pre” (predicted)
11 throughout the manuscript.

12

13 - You use very often "PRE" for Pearl River Estuary and CJE for "ChangJiang Estuary".
14 At least for the Figure captions, I would recommend to replace CJE by ChangJiang
15 Estuary, as it is not so obvious for most readers and it would make the Figure easier to
16 read.

17 [Response]: Accepted. Please see captions in Figs. 5, 7 and 8.

18

19

20

Tracing the origin of the oxygen-consuming organic matter in the hypoxic zone in a large eutrophic estuary: the lower reach of the Pearl River Estuary, China

Jianzhong Su¹, Minhan Dai^{1*}, Biyan He^{1,2}, Lifang Wang¹, Jianping Gan³,
Xianghui Guo¹, Huade Zhao¹ and Fengling Yu¹

¹State Key Laboratory of Marine Environmental Science, Xiamen University, Xiamen, China

²College of Food and Biological Engineering, Jimei University, Xiamen, China

³Department of Mathematics and Division of Environment, Hong Kong University of Science and Technology, Kowloon, Hong Kong, China

*Correspondence to: Minhan Dai (mdai@xmu.edu.cn)

Abstract. We assess the relative contributions of different sources of organic matter, marine vs. terrestrial, to oxygen consumption in an emerging hypoxic zone in the lower Pearl River Estuary (PRE), a large eutrophic estuary located in Southern China. Our cruise, conducted in July 2014, consisted of two legs before and after the passing of Typhoon Rammasun, which completely de-stratified the water column. The stratification recovered rapidly, within one day after the typhoon. We observed algal blooms in the upper layer of the water column and hypoxia underneath in bottom water during both legs. Repeat sampling at the initial hypoxic station showed severe oxygen depletion down to 30 $\mu\text{mol kg}^{-1}$ before the typhoon and a clear drawdown of dissolved oxygen after the typhoon. Based on a three end-member mixing model and the mass balance of dissolved inorganic carbon and its isotopic composition, the $\delta^{13}\text{C}$ of organic carbon remineralized in the hypoxic zone was -23.2 ± 1.1 ‰. We estimated that 65 ± 16 % of the oxygen-consuming organic matter was derived from marine sources, and the rest (35 ± 16 %) was derived from the continent. In contrast to a recently studied hypoxic zone in the East China Sea off the Changjiang Estuary where marine organic matter stimulated by eutrophication dominated oxygen consumption, here terrestrial organic matter significantly contributed to the formation and maintenance of hypoxia. How varying amounts of these organic matter sources drive oxygen consumption has important implications for better understanding hypoxia and its mitigation in bottom waters.

1 **1 Introduction**

2 The occurrence of hypoxia has been exacerbated worldwide (Nixon, 1995; Diaz and
3 Rosenberg, 2008; Rabalais et al., 2010; Zhang et al., 2013). In recent decades, more
4 than 400 coastal hypoxic systems have been reported with an exponential growth rate
5 of 5.5 ± 0.23 % yr⁻¹, demonstrating their persistence and complexity with respect to both
6 science and management (Diaz and Rosenberg, 2008; Vaquer-Sunyer and Duarte,
7 2008). Hypoxia may not only reduce biodiversity and endanger aquatic and benthic
8 habitats, but also alter the redox chemistry in both the water column and the underlying
9 sediments, triggering the release of secondary pollutants (Breitburg, 2002; Rutger et
10 al., 2002). Moreover, the management and recovery of these systems is complicated
11 due to the hysteresis of hypoxic conditions, and the varying timescales of biological
12 loss (within hours to weeks) and recovery from hypoxia (from months to years)
13 (Steckbauer et al., 2011).

14 Coastal hypoxia usually occurs in stratified water columns where the downward
15 mixing of oxygen from the surface is impeded (Kemp et al., 2009). Below the
16 pycnocline, aerobic respiration is usually the predominant sink of oxygen. Organic
17 matter, which consumes dissolved oxygen (DO) as it becomes oxidized, is thus the
18 ultimate cause of hypoxia under favourable physical settings (Rabouille et al., 2008;
19 Rabalais et al., 2014; Qian et al., 2016). The organic carbon (OC) that fuels
20 respiration-driven reduction of oxygen in these systems could originate from either
21 eutrophication-induced primary production (marine OC; OC_{mar}), or naturally and/or
22 anthropogenically driven delivery from terrestrial environments (terrestrial OC; OC_{terr})
23 (Paerl, 2006; Rabalais et al., 2010).

24 The question of how much OC in hypoxic zones is supplied from on-site primary
25 production versus the quantity derived from terrestrial sources has been an issue of
26 debate (Wang et al., 2016). Much of the phytoplankton-centric hypoxia literature
27 suggests that OC_{mar} dominates oxygen consumption in hypoxic zones, owing to its
28 higher microbial availability than OC_{terr} (Zimmerman and Canuel, 2000; Boesch et al.,
29 2009; Carstensen et al., 2014). Wang et al. (2016) quantified for the first time the
30 relative contributions of particulate OC_{mar} (POC_{mar}) and particulate OC_{terr} (POC_{terr}) in
31 consuming DO in the bottom waters of the East China Sea (ECS) off the Changjiang
32 Estuary (CJE), and found that POC_{mar} dominated DO consumption. However, other
33 studies suggest that POC_{terr} may also play an important role (Swarzenski et al., 2008;

1 Bianchi, 2011a; Bianchi et al., 2011b). It is thus very important to quantify the relative
2 contributions of organic matter (OC_{mar} vs. OC_{terr}) driving the onset and maintenance of
3 hypoxia in coastal systems, since reducing organic matter vs. nutrient inputs requires a
4 different set of management strategies.

5 The Pearl River Estuary (PRE, 21.2 °N–23.1 °N, 113.0 °E–114.5 °E) is surrounded
6 by several large cities including Hong Kong, Shenzhen and Guangzhou and has
7 received very high loads of nutrients from the drainage basin in the last three decades.
8 As such, eutrophication has increasingly become an issue of concern (Huang et al.,
9 2003; Ye et al., 2012). Dissolved inorganic nitrogen (DIN) concentrations in the PRE
10 have increased approximately 4-fold from 1986 ($19.3 \mu\text{mol L}^{-1}$) to 2002 ($76.1 \mu\text{mol}$
11 L^{-1}) (He and Yuan, 2007). This DIN increase has been attributed to increased inputs of
12 domestic sewage, industrial wastewater, agricultural runoff and aquaculture in the
13 watershed (Huang et al., 2003).

14 Recent observations based on monthly surveys between April 2010 and March 2011
15 and long term monitoring data from 1990 to 2014, have suggested that the lower PRE
16 has emerged as a seasonal hypoxic zone (Qian et al., 2017). This is supported by our
17 current study, as two relatively large hypoxic zones ($> 300 \text{ km}^2$) were observed in the
18 lower PRE with $\text{DO} < 2 \text{ mg L}^{-1}$. However, the origin of the organic matter driving
19 hypoxia in the lower PRE has not previously been examined. Here, we quantified the
20 relative proportions of OC_{mar} and OC_{terr} contributing to DO drawdown in bottom waters
21 of the lower PRE, an economically important coastal region. This study has important
22 biological, societal and managerial implications for the region, particularly relating to
23 water quality in the vicinity of Hong Kong in the lower PRE. For example, the
24 government of Hong Kong is examining the efficacy of its costly Harbour Area
25 Treatment Scheme project and if additional treatment should be implemented
26 (<http://www.gov.hk/en/residents/environment/water/harbourarea.htm>).

27 **2 Materials and Methods**

28 **2.1 Sampling and analysis**

29 Interrupted by Typhoon Rammasun on 17-18 July 2014, our cruise was divided into
30 two legs (Fig. 1). During Leg 1 on 13–16 July, we sampled Transects F4, F5 and
31 Stations A08–A18. During Leg 2 on 19–27 July, we sampled Stations A01–A10,
32 Transects F3 and F4, Stations A11–A17 and Transects F5, F6, F1, and F2, in sequence.

1 In order to monitor the development of hypoxia before and after the passage of the
2 typhoon, we revisited Station A10 three more times (13, 20 and 27 July).

3 According to the gauge in the upper Pearl River, water discharge peaked in June and
4 July. Typhoon Rammasun increased discharge during 15-18 July, with daily average
5 values of 19480, 26115, 22981 and 17540 m³ s⁻¹, respectively. Nevertheless, the
6 freshwater discharge was 18908 m³ s⁻¹ in leg 1 and 15698 m³ s⁻¹ in leg 2, comparable
7 to the long-term (2000–2011) monthly average.

8 Temperature and salinity were determined with a SBE 25
9 Conductivity-Temperature-Depth/Pressure unit (Sea-Bird Co.). Water samples were
10 collected using 4 L Go-Flo bottles (General Oceanics). DIC and DO was measured at
11 all stations with depth profiles. Samples for $\delta^{13}\text{C}_{\text{DIC}}$ were collected primarily along
12 Transect A as well as at depth in low oxygen layers.

13 The DO concentrations in discrete water samples were measured on board within 8 h
14 using the classic Winkler titration method (Dai et al., 2006). **In addition, we conducted**
15 **on-deck incubation experiments using unfiltered water taken from the hypoxic zone**
16 **on 27 July, 2014 following He et al. (2014). Bottom water from ~2 m above the**
17 **sediment surface was collected and incubated for 24 hours in 65 mL BOD bottles in**
18 **dark at ambient temperature controlled by the flowing surface water. Total oxygen**
19 **consumption rate was determined by comparing the DO concentration at the initial**
20 **and end point of the experiment.**

21 DIC was measured with an infrared detector after acidifying 0.5–0.7 mL of water
22 sample with a precision of 0.1 % for estuarine and sea waters (Cai et al., 2004).
23 Dissolved calcium concentrations (Ca²⁺) were determined using an EGTA titration
24 with a Metrohm 809 TITRANDO potentiometer, which has a precision better than ± 5
25 $\mu\text{mol kg}^{-1}$ (Cao et al., 2011).

26 For $\delta^{13}\text{C}_{\text{DIC}}$ analysis, an ~20 mL DIC sample was converted into gaseous CO₂ and
27 progressively purified through a vacuum line. The pure CO₂ sample was analyzed with
28 an isotope ratio mass spectrometer (IRMS, Finnigan MAT 252, Bremen, Germany).
29 The analytical precision was better than 0.1 ‰.

30 Water samples for TSM (total suspended matter), POC and $\delta^{13}\text{C}_{\text{POC}}$ analysis were
31 concentrated onto preweighed and pre-combusted 0.7 μm Whatman GF/F filters after
32 filtering 0.2–1.0 L of water under a mild vacuum (~ 25 kPa). Filters were washed with
33 distilled water and stored at -20 °C. Prior to analysis, all filters were freeze-dried. TSM

1 was determined using the net weight increment on the filter and the filtration volume.
 2 Filters were decarbonated with 1.0 mol L⁻¹ HCl and dried at 40 °C for 48 h (Kao et al.,
 3 2012) and analyzed for POC and δ¹³C_{POC} on an elemental analyzer coupled with an
 4 IRMS (EA-IRMS). The analytical precision for δ¹³C_{POC} was better than 0.1 ‰. Chl-a
 5 was measured with a Turner fluorometer after extracting filters with 90 % acetone (He
 6 et al., 2010b). Calibrations were performed using a Sigma Chl-a standard.

7 **2.2 Three end-member mixing model**

8 We adopted a three end-member mixing model to construct the conservative mixing
 9 scheme among different water masses (Cao et al., 2011; Han et al., 2012):

$$10 \quad F_{RI} + F_{SW} + F_{SUB} = 1 \quad (1)$$

$$11 \quad \theta_{RI} \times F_{RI} + \theta_{SW} \times F_{SW} + \theta_{SUB} \times F_{SUB} = \theta \quad (2)$$

$$12 \quad S_{RI} \times F_{RI} + S_{SW} \times F_{SW} + S_{SUB} \times F_{SUB} = S \quad (3)$$

13 where θ and S represent potential temperature and salinity; the subscripts RI, SW, and
 14 SUB denote the three different water masses (Pearl River plume water, offshore surface
 15 seawater and upwelled subsurface water); and F_{RI} , F_{SW} , and F_{SUB} represent the
 16 fractions that each end-member contributes to the in situ samples. These fractions were
 17 applied to predict **conservative** concentrations of DIC (DIC_{con}) and its isotopic
 18 composition ($\delta^{13}C_{DICcon}$) resulting solely from conservative mixing.

$$19 \quad DIC_{RI} \times F_{RI} + DIC_{SW} \times F_{SW} + DIC_{SUB} \times F_{SUB} = DIC_{con} \quad (4)$$

$$20 \quad \frac{\delta^{13}C_{DICRI} \times DIC_{RI} \times F_{RI} + \delta^{13}C_{DICSW} \times DIC_{SW} \times F_{SW} + \delta^{13}C_{DICSUB} \times DIC_{SUB} \times F_{SUB}}{DIC_{con}} = \delta^{13}C_{DICcon} \quad (5)$$

21 The difference (Δ) between measured and **conservative** DIC values represents the
 22 magnitude of the biological alteration of DIC (Wang et al., 2016).

23 **3 Results**

24 **3.1 Horizontal distribution**

25 Although the average freshwater discharge rate during our sampling period (16369 m³
 26 s⁻¹) was slightly higher than the multi-year (2000–2011) monthly average (15671 m³
 27 s⁻¹), typhoon Rammasun modified the system to some extent as shown from the
 28 evolution of chemical species at Station A10 before and after the typhoon (See Sect.
 29 3.4). The interruption of Leg 1 due to the typhoon (July 17-18) led to a smaller survey
 30 area, covering only outside Lingdingyang Bay (traditionally regarded as the PRE),

1 while Leg 2 covered Lingdingyang Bay from the Humen Outlet to the adjacent coastal
2 sea.

3 As depicted in Fig. 2, the sea surface temperature (SST) during Leg 1 (28.9-32.2 °C)
4 was slightly higher than during Leg 2 (28.9-31.0 °C). Sea surface salinity (SSS)
5 measurements showed that plume water was restricted more landward during Leg 2
6 than Leg 1. However, a steeper gradient to higher SST offshore during Leg 1 was
7 likely induced by the upwelling of bottom water, featuring relatively high SSS (18.6),
8 high DIC (1789 $\mu\text{mol kg}^{-1}$) and low DO saturation (DO%, 86 %). During Leg 1, the
9 region with the most productivity was found east of the Wanshan Islands, characterized
10 by high concentrations of Chl-a (8.0 $\mu\text{g kg}^{-1}$), low concentrations of DIC (1607 μmol
11 kg^{-1}), and DO supersaturation, with the highest DO% greater than 160 % at Station
12 F503. During Leg 2, there were three patches of high productivity, south of
13 Huangmaohai, at the PRE entrance, and off Hong Kong. The central region of high
14 productivity had the highest DO%, greater than 140% at Station A14, and was
15 characterized by relatively high concentrations of Chl-a (7.8 $\mu\text{g kg}^{-1}$) and low
16 concentrations of DIC (1737 $\mu\text{mol kg}^{-1}$).

17 As shown in Fig. 3, bottom water hypoxia during Leg 1 was located more centrally in
18 the study area relative to the surface phytoplankton bloom. The center of the hypoxic
19 zone was found at Station A10, characterized by the lowest observed DO
20 concentrations (as low as 30 $\mu\text{mol kg}^{-1}$) and a relatively high concentration of DIC
21 (2075 $\mu\text{mol kg}^{-1}$). During Leg 2, hypoxic conditions were no longer found at Station
22 A10, and instead the largest hypoxic zone was discovered to the southwest of the
23 Wanshan Islands, where the lowest DO values were observed (as low as 7 $\mu\text{mol kg}^{-1}$ at
24 F304), and once again coincided with relatively high concentrations of DIC (2146 μmol
25 kg^{-1}). We were unable to precisely constrain the areas of the regions impacted by
26 bottom water hypoxia due to the limited spatial coverage, but our results suggest it
27 covered an area of $> 280 \text{ km}^2$ during Leg 1 and $> 290 \text{ km}^2$ during Leg 2 according to
28 the definition of hypoxia as $\text{DO} < 2 \text{ mg L}^{-1}$ or 63 μM , or an area of $> 900 \text{ km}^2$ during
29 Leg 1 and $> 800 \text{ km}^2$ during Leg 2 assuming the threshold of the oxygen-deficit zone
30 was $< 3 \text{ mg L}^{-1}$ or 95 μM (Rabalais et al., 2010; Zhao et al., 2017).

1 **3.2 Vertical distribution**

2 During Leg 1, plume water reached 50 km offshore from the entrance of the PRE,
3 forming a 5–10 m thick surface layer (Fig. 4b). Both the thermocline and halocline
4 contributed to the stability of the water column structure, which favored the formation
5 of bottom water hypoxia. The thickness of the bottom water hypoxic layer was ~ 5 m.
6 The region of highest productivity, however, was not observed in the same location as
7 the hypoxic zone, but further offshore.

8 During Leg 2, although the passing of the typhoon would be expected to absorb large
9 amounts of potential heat and cause extensive mixing of the water column, the
10 enhanced freshwater discharge could rapidly re-stratify the water column and facilitate
11 the re-formation of hypoxia. This time, the primary region of hypoxia was observed
12 directly below the bloom, with a thickness of 3 m (Fig. 4i). Additionally, near the
13 Humen Outlet we observed low DIC (1466 $\mu\text{mol kg}^{-1}$) and moderately low DO (89
14 $\mu\text{mol kg}^{-1}$), which reflected the input of the low DO water mass from upstream as
15 reported previously (Dai et al., 2006; Dai et al., 2008a; He et al., 2014).

16 **3.3 Isotopic composition of DIC and POC**

17 The $\delta^{13}\text{C}$ values of DIC became progressively heavier from stations dominated by
18 freshwater (~ -11.4 ‰) to off-shore seawater (~ -0.6 ‰), with a relatively wide range of
19 values beyond a salinity of 13 (Fig. 5). Owing to a malfunction of the instrument,
20 $\delta^{13}\text{C}_{\text{POC}}$ data from our cruise were not available. Instead, we reported a valid $\delta^{13}\text{C}_{\text{POC}}$
21 dataset from a 2015 summer cruise in approximately the same region. $\delta^{13}\text{C}_{\text{POC}}$ values
22 showed a similar trend with $\delta^{13}\text{C}_{\text{DIC}}$, i.e. ^{13}C enriched seaward, from ~ -28 ‰ to ~ -20
23 ‰. In the bloom, where the DO% was above 125 %, the mean $\delta^{13}\text{C}$ value for POC
24 was -19.4 ± 0.8 ‰ (n=8), which was within the typical range of marine phytoplankton
25 (Peterson and Fry, 1987). As shown in Fig. 5, there was a large $\delta^{13}\text{C}_{\text{POC}}$ decrease near a
26 salinity of 15. Geographically, it was located at the mixing dominated zone in inner
27 Lingdingyang Bay, where intense resuspension of ^{13}C depleted sediments may occur
28 (Guo et al., 2009).

29 **3.4 Reinstatement of the hypoxic station after Typhoon Rammasun**

30 Typhoon Rammasun made landfall at Zhanjiang, located 400 km to the southwest of
31 the PRE, at 20:00 LT (Local Time) on 18 July, and was dissipated by 05:00 LT on 20

1 July. The typhoon completely de-stratified the water column during its passing.
2 However, the associated heavy precipitation and runoff appeared to re-establish
3 stratification rather quickly, within one day, as suggested by the salinity gradient (18–
4 30) from 0–10 m depth during Leg 2 at 15:20 LT on 20 July (Fig. 6b). In order to
5 capture the evolution of DO between the disruption and reinstatement of stratification,
6 we resumed our cruise and revisited Station A10 (Fig. 6). On 13 July, the bottom water
7 at Station A10 was the hypoxic core, with the lowest observed DO ($30 \mu\text{mol kg}^{-1}$) and
8 highest DIC ($2075 \mu\text{mol kg}^{-1}$) concentrations. On 20 July, the results showed that the
9 temperature homogeneous layer in the bottom water (9–13 m) might reflect the
10 remnants of typhoon-induced mixing (Fig. 6a), while the reduction in salinity at <9 m
11 depicted the rapid re-establishment of stratification as a result of enhanced freshwater
12 discharge (Fig. 6b). Bottom water DO increased to $153 \mu\text{mol kg}^{-1}$ and DIC decreased to
13 $1901 \mu\text{mol kg}^{-1}$ as a result of the typhoon-induced water column mixing and aeration. In
14 addition, TSM increased sharply from 20.2 before the typhoon to 36.6 mg kg^{-1} ,
15 suggesting large volumes of sediment had been resuspended during its passing. On 27
16 July, one week after the typhoon, strong thermohaline stratification was re-established
17 in the whole water column. Along with the intensifying stratification, bottom water DO
18 decreased to $99 \mu\text{mol kg}^{-1}$ indicating continuous DO depletion and the potential for
19 hypoxia formation. Meanwhile, bottom water DIC concentrations increased to 2000
20 $\mu\text{mol kg}^{-1}$ and dissolved inorganic phosphate (DIP) rose from 0.28 to $0.57 \mu\text{mol kg}^{-1}$.
21 Moreover, bottom-water TSM returned to pre-typhoon (13 July) levels.

22 **4 Discussion**

23 **4.1 Selection of end-members and model validation**

24 The potential temperature-salinity plot displayed a three end-member mixing scheme
25 over the PRE and adjacent coastal waters (Fig. 7a), consisting of Pearl River plume
26 water, offshore surface seawater and upwelled subsurface water. During the summer, a
27 DIC concentration of $\sim 1917 \mu\text{mol kg}^{-1}$ was observed at $S=33.7$, which can be regarded
28 as the offshore surface seawater end-member (Guo and Wong, 2015). Here, by
29 choosing $S=34.6$ as the offshore subsurface water salinity end-member, we obtained a
30 DIC value of $\sim 2023 \mu\text{mol kg}^{-1}$, similar to the value at ~ 100 m depth adopted by Guo
31 and Wong (2015). For the plume end-member, it was difficult to directly select from the

1 field data, because biological alteration might lead to altered values within the plume
2 influenced area. Therefore, we first assumed that the plume water observed on the shelf
3 consisted of a mixture of freshwater and offshore surface seawater. Then, we compiled
4 3 years of surface data from the summer (August 2012, July 2014 and July 2015) to
5 extrapolate the relatively stable freshwater end-member and examine the biological
6 effect on DIC-salinity relationships. By constraining DIC end-members (freshwater
7 and offshore surface seawater), we observed that DIC remained overall conservative
8 when salinity was <10.8 but showed removal when salinity was >10.8 (Han et al.,
9 2012). Thus, we derived plume end-member values ($1670 \pm 50 \mu\text{mol kg}^{-1}$) from the
10 DIC-salinity conservative mixing curve at $S=10.8$. Furthermore, $S=10.8$ was observed
11 at the innermost station (A08) during Leg 1, which agreed well with the spatial and
12 temporal scale of the actual water mass mixing in our survey. To confirm our results,
13 we also used a freshwater end-member ($S=0$), but the output of the model showed little
14 difference from that based on the plume end-member at $S=10.8$.

15 The $\delta^{13}\text{C}_{\text{DIC}}$ value was $0.6 \pm 0.2 \text{ ‰}$ in the offshore surface seawater at $S \sim 33.7$, where
16 nutrient ($\text{NO}_3^- + \text{NO}_2^-$ and DIP) concentrations were close to their detection limits and
17 DO was nearly saturated, indicating little biological activity. As DIC remained overall
18 conservative when salinity was < 10.8 , the $\delta^{13}\text{C}_{\text{DIC}}$ value of $-11.4 \pm 0.2 \text{ ‰}$ at $S < 0.4$ is
19 representative of the freshwater source. Assuming the plume water is a mixture of
20 freshwater and offshore surface seawater, the initial plume end-member of $\delta^{13}\text{C}_{\text{DIC}}$ at
21 $S=10.8$ can be calculated via an isotopic mass balance ($-7.0 \pm 0.8 \text{ ‰}$). A summary of the
22 end-member values used in this study is listed in Table 1.

23 We calculated the fractions of the three water masses based on potential temperature
24 and salinity equations, so as to predict conservative DIC (DIC_{con}) and its isotopic
25 composition ($\delta^{13}\text{C}_{\text{DICcon}}$) solely from conservative mixing. We chose the concentration
26 of Ca^{2+} as a conservative tracer to validate our model prediction, assuming CaCO_3
27 precipitation or dissolution is not significant. This assumption is supported by a strong
28 linear relationship between surface water Ca^{2+} and salinity, and aragonite
29 oversaturation ($\Omega_{\text{arag}} = 2.6 \pm 0.7$) in the subsurface water. Our model derived values
30 were in good accordance with the field-observed values (Fig. 7b), which strongly
31 supported our model prediction.

32 As shown in Fig. 7c, most of the observed DIC concentrations in the subsurface water
33 were higher than the conservative values, as a result of DIC production via OC

1 oxidation. This coincided with lighter $\delta^{13}\text{C}_{\text{DIC}}$ values than **conservative**, owing to the
 2 accumulation of isotopically lighter carbon entering the DIC pool from remineralized
 3 organic matter (Fig. 7d). Based on the differences between the observed and
 4 **conservative** values of DIC and $\delta^{13}\text{C}_{\text{DIC}}$, the carbon isotopic composition of the
 5 oxygen-consuming organic matter could be traced precisely (see details in Sect. 4.2).

6 In the subsurface water, the bulk of ΔDIC values varied from 0 to **132** $\mu\text{mol kg}^{-1}$,
 7 coupled with a range of apparent oxygen utilization (AOU) values from 0 to **179** μmol
 8 kg^{-1} . ΔDIC values positively correlated with AOU (Fig. 7e), corresponding to the fact
 9 that the additional DIC was supplied by organic matter remineralization via aerobic
 10 respiration. The slope of ΔDIC vs. AOU in the subsurface water was 0.71 ± 0.03 , which
 11 agrees well with classic Redfield stoichiometry (i.e., $106/138=0.77$), providing further
 12 evidence for aerobic respiration as the source of added DIC. **As a first order**
 13 **comparison, the water column total oxygen consumption rate of $9.8 \mu\text{mol L}^{-1} \text{d}^{-1}$ could**
 14 **well support the oxygen decline rate observed at Station A10 in the hypoxic zone**
 15 **between 20 July and 27 July (Fig. 6), which was $7.7 \mu\text{mol L}^{-1} \text{d}^{-1}$. This comparison**
 16 **along with the stoichiometry between ΔDIC and AOU strongly suggests that water**
 17 **column aerobic respiration may be predominate in the formation of the hypoxia in the**
 18 **present case.**

19 **4.2 Isotopic composition of the oxygen-consuming OC**

20 The DIC isotopic mass balance is shown in Eq. (6) (Wang et al., 2016):

$$21 \quad \delta^{13}\text{C}_{\text{DICobs}} \times \text{DIC}_{\text{obs}} = \delta^{13}\text{C}_{\text{DICcon}} \times \text{DIC}_{\text{con}} + \delta^{13}\text{C}_{\text{DICbio}} \times \text{DIC}_{\text{bio}} \quad (6)$$

22 where the subscripts obs, **con** and bio refer to the field-observed, **conservative** and
 23 biologically altered values.

24 Degradation of OC typically produces DIC with minor isotopic fractionation from
 25 the OC substrate (Hullar et al., 1996; Breteler et al., 2002). Thus, the isotopic
 26 composition of DIC_{bio} (i.e., $\delta^{13}\text{C}_{\text{DICbio}}$) should be identical to the $\delta^{13}\text{C}$ of the OC
 27 ($\delta^{13}\text{C}_{\text{OCx}}$), which consumed oxygen and produced DIC_{bio} . $\delta^{13}\text{C}_{\text{OCx}}$ was derived from the
 28 mass balance equations of both DIC and its stable isotope:

$$29 \quad \delta^{13}\text{C}_{\text{OCx}} = \frac{\delta^{13}\text{C}_{\text{obs}} \times \text{DIC}_{\text{obs}} - \delta^{13}\text{C}_{\text{con}} \times \text{DIC}_{\text{con}}}{\text{DIC}_{\text{obs}} - \text{DIC}_{\text{con}}} \quad (7)$$

30 Equation (7) can be rearranged into Eq. (8):

$$31 \quad \Delta(\delta^{13}\text{C}_{\text{DIC}} \times \text{DIC}) = \delta^{13}\text{C}_{\text{OCx}} \times \Delta\text{DIC} \quad (8)$$

1 As shown in Fig. 8, the slope of the linear regression represents $\delta^{13}\text{C}_{\text{OCx}}$ or $\delta^{13}\text{C}_{\text{DICbio}}$,
2 which here is equal to -23.2 ± 1.1 ‰. This value reflects the original $\delta^{13}\text{C}$ signature of
3 the remineralized organic matter contributing to the observed addition of DIC.

4 Although studies have shown selective diagenesis of isotopically heavy or light pools
5 of organic matter (Marthur et al., 1992; Lehmann et al., 2002), these effects are small
6 compared to the isotopic differences among different sources of organic matter
7 (Meyers, 1997). It is thus reasonable to assume that the isotopic ratios are conservative
8 and that physical mixing of the end-member sources determine the isotopic
9 composition of organic matter in natural systems (Gearing et al., 1984; Cifuentes et al.,
10 1988; Thornton and McManus, 1994). The relative contributions of marine and
11 terrestrial sources to oxygen-consuming organic matter in our study area could be
12 estimated based on the following equation (Shultz and Calder, 1976; Hu et al., 2006):

$$13 \quad f(\%) = \frac{\delta^{13}\text{C}_{\text{mar}} - \delta^{13}\text{C}_{\text{OCx}}}{\delta^{13}\text{C}_{\text{mar}} - \delta^{13}\text{C}_{\text{terr}}} \times 100 \quad (9)$$

14 Here, for the terrestrial end-member ($\delta^{13}\text{C}_{\text{terr}}$), we adopted the average $\delta^{13}\text{C}$ value of
15 POC sampled near the Humen Outlet ($S < 4$), which represents the predominant source
16 of riverine material entering the estuary (He et al., 2010b). The mean $\delta^{13}\text{C}_{\text{POC}}$ value,
17 -28.3 ± 0.7 ‰ ($n=7$), is very similar to the freshwater $\delta^{13}\text{C}_{\text{POC}}$ value of -28.7 ‰
18 reported by Yu et al. (2010), which reflected a terrigenous mixture of C3 plant
19 fragments and forest soils. For the marine end-member ($\delta^{13}\text{C}_{\text{mar}}$), we calculated the
20 mean surface water $\delta^{13}\text{C}_{\text{POC}}$ value (-19.4 ± 0.8 ‰, $n=8$) from stations with $S > 26$ where
21 significant phytoplankton blooms were observed, as indicated by DO supersaturation
22 ($\text{DO}\% > 125$ ‰) and relatively high pH values (> 8.3) and POC contents (5.3 ± 2.4 ‰).
23 This value is similar, although slightly heavier than the marine end-member used by
24 Chen et al. (2008), who measured a $\delta^{13}\text{C}$ value of -20.9 ‰ in tow-net phytoplankton
25 samples from outer Lingdingyang Bay, in the same region as this study. Additionally,
26 He et al. (2010a) reported a $\delta^{13}\text{C}$ value of -20.8 ± 0.4 ‰ in phytoplankton collected
27 from the northern South China Sea. These values are consistent enough for us to
28 compile and use an average $\delta^{13}\text{C}_{\text{mar}}$ value of -20.5 ± 0.9 ‰. This value agrees well
29 with the reported stable carbon isotopic signature of marine organic matter in other
30 coastal regions. For example, mean isotopic values of phytoplankton were reported as
31 -20.3 ± 0.6 ‰ in Narragansett Bay (Gearing et al., 1984), -20.3 ± 0.9 ‰ in Auke Bay

1 and Fritz Cove (Goering et al., 1990), and -20.1 ± 0.8 ‰ in the Gulf of Lions
2 (Harmelin-Vivien et al., 2008).

3 Our model results suggest that marine organic matter contributed to 65 ± 16 % of the
4 observed oxygen consumption, while terrestrial organic matter accounted for the
5 remaining 35 ± 16 %. It is thus clear that marine organic matter from
6 eutrophication-induced primary production dominated oxygen consumption in the
7 hypoxic zone; however, terrestrial organic matter also contributed significantly to the
8 formation and maintenance of hypoxia in the lower PRE and adjacent coastal waters.

9 **4.3 Comparison with hypoxia in the East China Sea off the Changjiang Estuary**

10 As one of the largest rivers in the world, the Changjiang has been suffering from
11 eutrophication for the past few decades (Zhang et al., 1999; Wang et al., 2014). In
12 summer, sharp density gradients with frequent algal blooms and subsequent organic
13 matter decomposition cause seasonal hypoxia in the bottom water of the ECS off the
14 CJE. Wang et al. (2016) revealed that the remineralization of marine organic matter
15 (OC_{mar}) overwhelmingly (nearly 100 %) contributed to DO consumption in the ECS off
16 the CJE. However, our present study showed that less OC_{mar} contributed to the oxygen
17 depletion (65 ± 16 %) in the hypoxic zone of the lower PRE.

18 As shown in Fig. 5, there is little difference between $\delta^{13}C_{\text{DIC}}$ and $\delta^{13}C_{\text{POC}}$ values of
19 the marine end-member. However, the $\delta^{13}C_{\text{DIC}}$ and $\delta^{13}C_{\text{POC}}$ values of the freshwater
20 end-member showed some dissimilarity, with lighter values in the PRE (-11.4 ± 0.2 ‰,
21 -28.3 ± 0.7 ‰) than in the CJE (-8.8 ‰, -24.4 ± 0.2 ‰). In Fig. 7e, the amplitude of
22 ΔDIC and AOU values suggest a similar intensity of OM biodegradation, and the
23 slope of ΔDIC vs. AOU (0.71 ± 0.03 vs. 0.65 ± 0.04) indicates a predominance of
24 aerobic respiration in the two systems. As seen from Table 2, there is no significant
25 difference between the $\delta^{13}C$ values of surface sediments within the hypoxic zones of
26 the PRE and CJE. However, data in Fig. 7a show generally higher water temperatures
27 in the PRE than in the CJE. For instance, the temperature of surface and subsurface
28 seawater end-members in the PRE is 2-3 °C higher than in the CJE. From a spatial
29 point of view, the distance from the river mouth to the hypoxic zone in the CJE is 2-3
30 times longer than in the PRE, possibly resulting in a longer travel time of OC_{terr} .
31 Therefore, we contend that the difference in the predicted distributions of marine and
32 terrestrial sources of organic matter contributing to oxygen consumption in and off the

1 PRE and CJE is likely related to differences in the bioavailability of OC_{terr} and OC_{mar} ,
2 the microbial community structures and the physical settings between these two
3 hypoxic systems.

4 Although C3 plants dominate and C4 plants are minor in both the Pearl River and
5 Changjiang drainage basins (Hu et al., 2006; Zhu et al., 2011a), the OC_{terr} delivered
6 from these two watersheds experiences varying degrees of degradation within the
7 estuaries before being transported into the coastal hypoxic zones. In the CJE,
8 approximately 50 % of OC_{terr} becomes remineralized during transport through the
9 estuary, likely due to efficient OM unloading from mineral surfaces (Zhu et al., 2011a)
10 and longer residence times within the estuary, facilitating microbial transformation and
11 degradation. In contrast, the PRE appears to be a somewhat intermediate site with the
12 export of OC_{terr} being closely associated with sedimentary regimes and not
13 characterized by extensive degradative loss (Strong et al., 2012). Thus, the
14 bioavailability of OC_{terr} that reached the hypoxic zone is likely higher in the PRE than
15 in the CJE. Moreover, the increased precipitation and runoff during the typhoon may
16 have mobilized additional fresh anthropogenic OM from surrounding megacities (e.g.
17 Guangzhou, Shenzhen and Zhuhai) deposited in the river channel, which could lead to
18 more labile OC_{terr} in the PRE. Additionally, the difference in bacterial community
19 structure between the two systems may have played a role. Recent studies have
20 demonstrated that the bacterial community in the PRE is characterized by higher
21 relative abundances of Actinobacteria and lower relative abundances of
22 Cytophaga-Flavobacteria-Bacteroides (CFB) than in the CJE (Liu et al., 2012; Zhang et
23 al., 2016). Whether such differences would promote the degradation of OC_{terr} in the
24 PRE relative to the CJE remains unknown. Finally, the temperature of the bottom water
25 in the PRE hypoxic zone (27–29 °C) was higher than in the CJE hypoxic zone (21.5–
26 24.0 °C), which may have accelerated the rates of bacterial growth and OM
27 decomposition (Brown et al., 2004).

28 **5 Conclusions**

29 Based on a three end-member mixing model and the mass balance of DIC and its
30 isotopic composition, we demonstrated that the organic matter decomposed via aerobic
31 respiration in the stratified subsurface waters of the lower PRE and adjacent coastal
32 waters was predominantly OC_{mar} (49-81 %, mean 65 %), with a significant portion of

1 OC_{terr} also decomposed (19-51 %, mean 35 %). The relative distribution of organic
2 matter sources contributing to oxygen drawdown differs in the hypoxic zone off the
3 CJE, where it is caused almost entirely by OC_{mar}. These differences have important
4 implications for better understanding the controls on hypoxia and its mitigation.
5 Nevertheless, with respect to increasing coastal nutrient levels, a significant implication
6 of the present study is that reducing and managing nutrients is critical to control
7 eutrophication and, subsequently, to mitigate hypoxia (Conley et al., 2009; Paerl, 2009;
8 Mercedes et al., 2015; Stefan et al., 2016). Given that OC_{terr} also contributes to the
9 consumption of oxygen in the lower PRE hypoxic zone, it is crucial to characterize the
10 source of this oxygen-consuming terrestrial organic matter, whether from natural soil
11 leaching and/or anthropogenic wastewater discharge, so as to make proper policies for
12 hypoxia remediation.

13 The processes involved in the partitioning of organic matter sources, their isotopic
14 signals and their subsequent biogeochemical transformations in the PRE hypoxic zone
15 are illustrated in the conceptual diagram in Fig. 9. The river delivers a significant
16 amount of nutrients and terrestrial organic matter to the estuary, stimulating
17 phytoplankton blooms in the surface water at the lower reaches of the estuary where
18 turbidity is relatively low and conditions are favourable for phytoplankton growth
19 (Gaston et al., 2006; Dai et al., 2008b; Guo et al., 2009). The subsequent sinking of this
20 biomass along with terrestrial organic matter below the pycnocline consumes oxygen
21 and adds respired DIC to subsurface waters, resulting in coastal hypoxia. Therefore, we
22 conclude that within the PRE and adjacent coastal areas, the most important biological
23 process with respect to forming and maintaining hypoxic conditions is aerobic
24 respiration.

25

26

27

28 *Acknowledgments.* This research was funded by the National Natural Science
29 Foundation of China through grants 41130857, 41576085 and 41361164001. We thank
30 Tengxiang Xie, Li Ma, Shengyao Sun, Chenhe Zheng and Liangrong Zou for their
31 assistance in sample collections; Yan Li and Yawen Wei for providing the calcium
32 concentration data; Liguó Guo, Tao Huang and Dawei Li for assisting on the
33 measurements of DIC, nutrients and $\delta^{13}\text{C}_{\text{POC}}$. The captain and the crew of R/V *Kediao 8*

1 are acknowledged for their cooperation during the cruise. Finally, we express our
2 gratitude to two anonymous referees for their insightful and constructive comments and
3 input.

7 **References**

8 Bianchi, T. S.: The role of terrestrially derived organic carbon in the coastal ocean: A
9 changing paradigm and the priming effect, *Proc. Natl. Acad. Sci. U.S.A.*, 108,
10 19473-19481, doi:10.1073/pnas.1017982108, 2011a.

11 Bianchi, T. S., Wysocki, L. A., Schreiner, K. M., Filley, T. R., Corbett, D. R., and
12 Kolker, A. S.: Sources of terrestrial organic carbon in the Mississippi plume region:
13 evidence for the importance of coastal marsh inputs, *Aquat. Geochem.*, 17, 431-456,
14 doi:10.1007/s10498-010-9110-3, 2011b.

15 Boesch, D. F., Boynton, W. R., Crowder, L. B., Diaz, R. J., Howarth, R. W., Mee, L. D.,
16 Nixon, S. W., Rabalais, N. N., Rosenberg, R., Sanders, J. G., Scavia, D., and Turner,
17 R. E.: Nutrient Enrichment Drives Gulf of Mexico Hypoxia, *Eos, Trans. Amer.*
18 *Geophys. Union*, 90, 117-118, doi:10.1029/2009EO140001, 2009.

19 Breitburg, D.: Effects of hypoxia, and the balance between hypoxia and enrichment, on
20 coastal fishes and fisheries, *Estuaries*, 25, 767-781, doi:10.1007/BF02804904, 2002.

21 Breteler, W. C. K., Grice, K., Schouten, S., Kloosterhuis, H. T., and Damsté J. S. S.:
22 Stable carbon isotope fractionation in the marine copepod *Temora longicornis*:
23 unexpectedly low $\delta^{13}\text{C}$ value of faecal pellets, *Mar. Ecol. Prog. Ser.*, 240, 195-204,
24 doi:10.3354/meps240195, 2002.

25 Brown, J. H., Gillooly, J. F., Allen, A. P., Savage, V. M., and West, G. B.: Toward a
26 metabolic theory of ecology, *Ecology*, 85, 1771-1789, doi:10.1890/03-9000, 2004.

27 Cai, W.-J., Dai, M., Wang, Y., Zhai, W., Huang, T., Chen, S., Zhang, F., Chen, Z., and
28 Wang, Z.: The biogeochemistry of inorganic carbon and nutrients in the Pearl River
29 estuary and the adjacent Northern South China Sea, *Cont. Shelf Res.*, 24, 1301-1319,
30 doi:10.1016/j.csr.2004.04.005, 2004.

31 Cao, Z., Dai, M., Zheng, N., Wang, D., Li, Q., Zhai, W., Meng, F., and Gan, J.:
32 Dynamics of the carbonate system in a large continental shelf system under the

1 influence of both a river plume and coastal upwelling, *J. Geophys. Res. Biogeosci.*,
2 116, G02010, doi:10.1029/2010JG001596, 2011.

3 Carstensen, J., Andersen, J. H., Gustafsson, B. G., and Conley, D. J.: Deoxygenation of
4 the Baltic Sea during the last century, *Proc. Natl. Acad. Sci. U.S.A.*, 111, 5628-5633,
5 doi:10.1073/pnas.1323156111, 2014.

6 Chen, F., Zhang, L., Yang, Y., and Zhang, D.: Chemical and isotopic alteration of
7 organic matter during early diagenesis: Evidence from the coastal area off-shore the
8 Pearl River estuary, south China, *J. Mar. Syst.*, 74, 372-380,
9 doi:10.1016/j.jmarsys.2008.02.004, 2008.

10 Cifuentes, L., Sharp, J., and Fogel, M. L.: Stable carbon and nitrogen isotope
11 biogeochemistry in the Delaware estuary, *Limnol. Oceanogr.*, 33, 1102-1115,
12 doi:10.4319/lo.1988.33.5.1102, 1988.

13 Conley, D. J., Paerl, H. W., Howarth, R. W., Boesch, D. F., Seitzinger, S. P., Karl, E.,
14 Karl, E., Lancelot, C., Gene, E., and Gene, E.: Controlling eutrophication: nitrogen
15 and phosphorus, *Science*, 123, 1014-1015, doi:10.1126/science.1167755, 2009.

16 Dai, M., Guo, X., Zhai, W., Yuan, L., Wang, B., Wang, L., Cai, P., Tang, T., and Cai,
17 W.-J.: Oxygen depletion in the upper reach of the Pearl River estuary during a winter
18 drought, *Mar. Chem.*, 102, 159-169, doi:10.1016/j.marchem.2005.09.020, 2006.

19 Dai, M., Wang, L., Guo, X., Zhai, W., Li, Q., He, B., and Kao, S.-J.: Nitrification and
20 inorganic nitrogen distribution in a large perturbed river/estuarine system: the Pearl
21 River Estuary, China, *Biogeosciences*, 5, 1227-1244, doi:10.5194/bg-5-1227-2008,
22 2008a.

23 Dai, M., Zhai, W., Cai, W.-J., Callahan, J., Huang, B., Shang, S., Huang, T., Li, X., Lu,
24 Z., Chen, W., and Chen, Z.: Effects of an estuarine plume-associated bloom on the
25 carbonate system in the lower reaches of the Pearl River estuary and the coastal zone
26 of the northern South China Sea, *Cont. Shelf Res.*, 28, 1416-1423, doi:
27 10.1016/j.csr.2007.04.018, 2008b.

28 Diaz, R. J. and Rosenberg, R.: Spreading dead zones and consequences for marine
29 ecosystems, *Science*, 321, 926-929, doi:10.1126/science.1156401, 2008.

30 Gaston, T. F., Schlacher, T. A., and Connolly, R. M.: Flood discharges of a small river
31 into open coastal waters: Plume traits and material fate, *Estuar. Coast. Shelf Sci.*, 69,
32 4-9, doi:10.1016/j.ecss.2006.03.015, 2006.

- 1 Gearing, J. N., Gearing, P. J., Rudnick, D. T., Requejo, A. G., and Hutchins, M. J.:
2 Isotopic variability of organic carbon in a phytoplankton-based, temperate estuary,
3 *Geochim. Cosmochim. Acta*, 48, 1089-1098, doi:10.1016/0016-7037(84)90199-6,
4 1984.
- 5 Goering, J., Alexander, V., and Haubenstock, N.: Seasonal variability of stable carbon
6 and nitrogen isotope ratios of organisms in a North Pacific Bay, *Estuar. Coast. Shelf*
7 *Sci.*, 30, 239-260, doi:10.1016/0272-7714(90)90050-2, 1990.
- 8 Guo, X., Dai, M., Zhai, W., Cai, W.-J., and Chen, B.: CO² flux and seasonal variability
9 in a large subtropical estuarine system, the Pearl River Estuary, China, *J. Geophys.*
10 *Res. Biogeosci.*, 114, G03013, doi:10.1029/2008JG000905, 2009.
- 11 Guo, X. and Wong, G. T.: Carbonate chemistry in the northern South China Sea
12 shelf-sea in June 2010, *Deep-Sea Res. II*, 117, 119-130,
13 doi:10.1016/j.dsr2.2015.02.024, 2015.
- 14 Han, A., Dai, M., Kao, S.-J., Gan, J., Li, Q., Wang, L., Zhai, W., and Wang, L.: Nutrient
15 dynamics and biological consumption in a large continental shelf system under the
16 influence of both a river plume and coastal upwelling, *Limnol. Oceanogr.*, 57,
17 486-502, doi:10.4319/lo.2012.57.2.0486, 2012.
- 18 Harmelin-Vivien, M., Loizeau, V., Mellon, C., Beker, B., Arlhac, D., Bodiguel, X.,
19 Ferraton, F., Hermand, R., Philippon, X., and Salen-Picard, C.: Comparison of C and
20 N stable isotope ratios between surface particulate organic matter and
21 microphytoplankton in the Gulf of Lions (NW Mediterranean), *Cont. Shelf Res.*, 28,
22 1911-1919, 2008.
- 23 He, B., Dai, M., Huang, W., Liu, Q., Chen, H., and Xu, L.: Sources and accumulation of
24 organic carbon in the Pearl River Estuary surface sediment as indicated by elemental,
25 stable carbon isotopic, and carbohydrate compositions, *Biogeosciences*, 7,
26 3343-3362, doi:10.5194/bg-7-3343-2010, 2010a.
- 27 He, B., Dai, M., Zhai, W., Wang, L., Wang, K., Chen, J., Lin, J., Han, A., and Xu, Y.:
28 Distribution, degradation and dynamics of dissolved organic carbon and its major
29 compound classes in the Pearl River estuary, China, *Mar. Chem.*, 119, 52-64,
30 doi:10.1016/j.marchem.2009.12.006, 2010b.
- 31 He, B., Dai, M., Zhai, W., Guo, X., and Wang, L.: Hypoxia in the upper reaches of the
32 Pearl River Estuary and its maintenance mechanisms: A synthesis based on multiple

1 year observations during 2000–2008, *Mar. Chem.*, 167, 13-24,
2 doi:10.1016/j.marchem.2014.07.003, 2014.

3 He, G.-f. and Yuan, G.-m.: Assessment of the water quality by fuzzy mathematics for
4 last 20 years in Zhujiang Estuary, *Mar. Environ. Sci.*, 26, 53-57, 2007.

5 Hu, J., Peng, P. a., Jia, G., Mai, B., and Zhang, G.: Distribution and sources of organic
6 carbon, nitrogen and their isotopes in sediments of the subtropical Pearl River estuary
7 and adjacent shelf, Southern China, *Mar. Chem.*, 98, 274-285,
8 doi:10.1016/j.marchem.2005.03.008, 2006.

9 Huang, X., Huang, L., and Yue, W.: The characteristics of nutrients and eutrophication
10 in the Pearl River estuary, South China, *Mar. Pollut. Bull.*, 47, 30-36,
11 doi:10.1016/S0025-326X(02)00474-5, 2003.

12 Hullar, M., Fry, B., Peterson, B., and Wright, R.: Microbial utilization of estuarine
13 dissolved organic carbon: a stable isotope tracer approach tested by mass balance,
14 *Appl. Environ. Microbiol.*, 62, 2489-2493, 1996.

15 Kao, S.-J., Terence Yang, J.-Y., Liu, K.-K., Dai, M., Chou, W.-C., Lin, H.-L., and Ren,
16 H.: Isotope constraints on particulate nitrogen source and dynamics in the upper water
17 column of the oligotrophic South China Sea, *Global Biogeochem. Cycles*, 26,
18 GB2033, doi:10.1029/2011GB004091, 2012.

19 Kao, S. J., Lin, F. J., and Liu, K. K.: Organic carbon and nitrogen contents and their
20 isotopic compositions in surficial sediments from the East China Sea shelf and the
21 southern Okinawa Trough, *Deep Sea Res. Part II: Top. Stud. Oceanogr.*, 50,
22 1203-1217, doi:10.1016/S0967-0645(03)00018-3, 2003.

23 Kemp, W., Testa, J., Conley, D., Gilbert, D., and Hagy, J.: Temporal responses of
24 coastal hypoxia to nutrient loading and physical controls, *Biogeosciences*, 6,
25 2985-3008, doi:10.5194/bg-6-2985-2009, 2009.

26 Lehmann, M. F., Bernasconi, S. M., Barbieri, A., and McKenzie, J. A.: Preservation of
27 organic matter and alteration of its carbon and nitrogen isotope composition during
28 simulated and in situ early sedimentary diagenesis, *Geochim. Cosmochim. Acta*, 66,
29 3573-3584, doi:10.1016/S0016-7037(02)00968-7, 2002.

30 Li, D., Zhang, J., Huang, D., Wu, Y., and Liang, J.: Oxygen depletion off the
31 Changjiang (Yangtze River) estuary, *Sci. China Ser. D-Earth Sci.*, 45, 1137-1146,
32 doi:10.1360/02yd9110, 2002.

- 1 Liu, M., Xiao, T., Wu, Y., Zhou, F., Huang, H., Bao, S., and Zhang, W.: Temporal
2 distribution of bacterial community structure in the Changjiang Estuary hypoxia area
3 and the adjacent East China Sea, *Environ. Res. Lett.*, 7, 025001,
4 doi:10.1088/1748-9326/7/2/025001, 2012.
- 5 Marthur, J. M., Tyson, R. V., Thomson, J., and Matthey, D.: Early diagenesis of marine
6 organic matter: Alteration of the carbon isotopic composition, *Mar. Geol.*, 105,
7 51-61, doi:10.1016/0025-3227(92)90181-G, 1992.
- 8 Mercedes, M. C. B., Luiz Antonio, M., Tibisay, P., Rafael, R., Jean Pierre, H. B. O.,
9 Felipe Siqueira, P., Silvia Rafaela Machado, L., and Sorena, M.: Nitrogen
10 management challenges in major watersheds of South America, *Environ. Res. Lett.*,
11 10, 065007, doi:10.1088/1748-9326/10/6/065007, 2015.
- 12 Meyers, P. A.: Organic geochemical proxies of paleoceanographic, paleolimnologic,
13 and paleoclimatic processes, *Org. Geochem.*, 27, 213-250,
14 doi:10.1016/S0146-6380(97)00049-1, 1997.
- 15 Nixon, S. W.: Coastal marine eutrophication: A definition, social causes, and future
16 concerns, *Ophelia*, 41, 199-219, doi:10.1080/00785236.1995.10422044, 1995.
- 17 Paerl, H. W.: Assessing and managing nutrient-enhanced eutrophication in estuarine
18 and coastal waters: Interactive effects of human and climatic perturbations, *Ecol.*
19 *Eng.*, 26, 40-54, doi:10.1016/j.ecoleng.2005.09.006, 2006.
- 20 Paerl, H. W.: Controlling Eutrophication along the Freshwater–Marine Continuum:
21 Dual Nutrient (N and P) Reductions are Essential, *Estuar. Coast.*, 32, 593-601,
22 doi:10.1007/s12237-009-9158-8, 2009.
- 23 Peterson, B. J. and Fry, B.: Stable Isotopes in Ecosystem Studies, *Annu. Rev. Ecol.*
24 *Syst.*, 18, 293-320, 1987.
- 25 Qian, W., Dai, M., Xu, M., Kao, S.-j., Du, C., Liu, J., Wang, H., Guo, L., and Wang, L.:
26 Non-local drivers of the summer hypoxia in the East China Sea off the Changjiang
27 Estuary, *Estuar. Coast. Shelf Sci.*, doi:10.1016/j.ecss.2016.08.032, 2016.
- 28 Qian, W., Gan, J., Liu, J., He, B., Lu, Z., Guo, X., Wang, D., Guo, L., Huang, T., and
29 Dai, M.: Current status of emerging hypoxia in a large eutrophic estuary: the lower
30 reach of Pearl River estuary, China, Submitted to *Limnol. Oceanogr.*, 2017.
- 31 Rabalais, N., Cai, W.-J., Carstensen, J., Conley, D., Fry, B., Hu, X., Qui ñones-Rivera,
32 Z., Rosenberg, R., Slomp, C., Turner, E., Voss, M., Wissel, B., and Zhang, J.:

1 Eutrophication-Driven Deoxygenation in the Coastal Ocean, *Oceanography*, 27,
2 172-183, doi:10.5670/oceanog.2014.21, 2014.

3 Rabalais, N. N., D'áz, R. J., Levin, L. A., Turner, R. E., Gilbert, D., and Zhang, J.:
4 Dynamics and distribution of natural and human-caused hypoxia, *Biogeosciences*, 7,
5 585-619, doi:10.5194/bg-7-585-2010, 2010.

6 Rabouille, C., Conley, D. J., Dai, M. H., Cai, W. J., Chen, C. T. A., Lansard, B., Green,
7 R., Yin, K., Harrison, P. J., Dagg, M., and McKee, B.: Comparison of hypoxia among
8 four river-dominated ocean margins: The Changjiang (Yangtze), Mississippi, Pearl,
9 and Rhône rivers, *Cont. Shelf Res.*, 28, 1527-1537, doi:10.1016/j.csr.2008.01.020,
10 2008.

11 Rutger, R., Stefan, A., Birthe, H., Hans, C. N., and Karl, N.: Recovery of marine
12 benthic habitats and fauna in a Swedish fjord following improved oxygen conditions,
13 *Mar. Ecol. Prog. Ser.*, 234, 43-53, doi:10.3354/meps234043, 2002.

14 Shultz, D. J. and Calder, J. A.: Organic carbon $^{13}\text{C}/^{12}\text{C}$ variations in estuarine
15 sediments, *Geochim. Cosmochim. Acta*, 40, 381-385,
16 doi:10.1016/0016-7037(76)90002-8, 1976.

17 Steckbauer, A., Duarte, C. M., Carstensen, J., Vaquer-Sunyer, R., and Conley, D. J.:
18 Ecosystem impacts of hypoxia: thresholds of hypoxia and pathways to recovery,
19 *Environ. Res. Lett.*, 6, 025003, doi:10.1088/1748-9326/6/2/025003, 2011.

20 Stefan, R., Mateete, B., Clare, M. H., Nancy, K., Wilfried, W., Xiaoyuan, Y., Albert,
21 B., and Mark, A. S.: Synthesis and review: Tackling the nitrogen management
22 challenge: from global to local scales, *Environ. Res. Lett.*, 11, 120205,
23 doi:10.1088/1748-9326/11/12/120205, 2016.

24 Strong, D. J., Flecker, R., Valdes, P. J., Wilkinson, I. P., Rees, J. G., Zong, Y. Q., Lloyd,
25 J. M., Garrett, E., and Pancost, R. D.: Organic matter distribution in the modern
26 sediments of the Pearl River Estuary, *Org. Geochem.*, 49, 68-82,
27 doi:10.1016/j.orggeochem.2012.04.011, 2012.

28 Swarzenski, P., Campbell, P., Osterman, L., and Poore, R.: A 1000-year sediment
29 record of recurring hypoxia off the Mississippi River: The potential role of
30 terrestrially-derived organic matter inputs, *Mar. Chem.*, 109, 130-142,
31 doi:10.1016/j.marchem.2008.01.003, 2008.

- 1 Tan, F. C., Cai, D. L., and Edmond, J. M.: Carbon isotope geochemistry of the
2 Changjiang estuary, *Estuar. Coast. Shelf Sci.*, 32, 395-403,
3 doi:10.1016/0272-7714(91)90051-C, 1991.
- 4 Thornton, S. F. and McManus, J.: Application of Organic Carbon and Nitrogen Stable
5 Isotope and C/N Ratios as Source Indicators of Organic Matter Provenance in
6 Estuarine Systems: Evidence from the Tay Estuary, Scotland, *Estuar. Coast. Shelf
7 Sci.*, 38, 219-233, doi:10.1006/ecss.1994.1015, 1994.
- 8 Vaquer-Sunyer, R. and Duarte, C. M.: Thresholds of hypoxia for marine biodiversity,
9 *Proc. Natl. Acad. Sci. U.S.A.*, 105, 15452-15457, doi:10.1073/pnas.0803833105,
10 2008.
- 11 Wang, H., Dai, M., Liu, J., Kao, S.-J., Zhang, C., Cai, W.-J., Wang, G., Qian, W., Zhao,
12 M., and Sun, Z.: Eutrophication-Driven Hypoxia in the East China Sea off the
13 Changjiang Estuary, *Environ. Sci. Technol.*, 50, 2255-2263,
14 doi:10.1021/acs.est.5b06211, 2016.
- 15 Wang, Q., Koshikawa, H., Liu, C., and Otsubo, K.: 30-year changes in the nitrogen
16 inputs to the Yangtze River Basin, *Environ. Res. Lett.*, 9, 115005,
17 doi:10.1088/1748-9326/9/11/115005, 2014.
- 18 Xing, L., Zhang, H., Yuan, Z., Sun, Y., and Zhao, M.: Terrestrial and marine biomarker
19 estimates of organic matter sources and distributions in surface sediments from the
20 East China Sea shelf, *Cont. Shelf Res.*, 31, 1106-1115,
21 doi:10.1016/j.csr.2011.04.003, 2011.
- 22 Yao, P., Zhao, B., Bianchi, T. S., Guo, Z., Zhao, M., Li, D., Pan, H., Wang, J., Zhang,
23 T., and Yu, Z.: Remineralization of sedimentary organic carbon in mud deposits of
24 the Changjiang Estuary and adjacent shelf: Implications for carbon preservation and
25 authigenic mineral formation, *Cont. Shelf Res.*, 91, 1-11,
26 doi:10.1016/j.csr.2014.08.010, 2014.
- 27 Ye, F., Huang, X., Zhang, X., Zhang, D., Zeng, Y., and Tian, L.: Recent oxygen
28 depletion in the Pearl River Estuary, South China: geochemical and microfaunal
29 evidence, *J. Oceanogr.*, 68, 387-400, doi:10.1007/s10872-012-0104-1, 2012.
- 30 Yu, F., Zong, Y., Lloyd, J. M., Huang, G., Leng, M. J., Kendrick, C., Lamb, A. L., and
31 Yim, W. W.-S.: Bulk organic $\delta^{13}\text{C}$ and C/N as indicators for sediment sources in the
32 Pearl River delta and estuary, southern China, *Estuar. Coast. Shelf Sci.*, 87, 618-630,
33 doi:10.1016/j.ecss.2010.02.018, 2010.

1 Zhang, J., Zhang, Z. F., Liu, S. M., Wu, Y., Xiong, H., and Chen, H. T.: Human impacts
2 on the large world rivers: Would the Changjiang (Yangtze River) be an illustration?,
3 *Global Biogeochem. Cycles*, 13, 1099-1105, doi:10.1029/1999GB900044, 1999.

4 Zhang, J., Cowie, G., and Naqvi, S. W. A.: Hypoxia in the changing marine
5 environment, *Environ. Res. Lett.*, 8, 015025, doi:10.1088/1748-9326/8/1/015025,
6 2013.

7 Zhang, Y., Xiao, W., and Jiao, N.: Linking biochemical properties of particles to
8 particle-attached and free-living bacterial community structure along the particle
9 density gradient from freshwater to open ocean, *J. Geophys. Res. Biogeosci.*, 121,
10 2261-2274, doi:10.1002/2016JG003390, 2016.

11 Zhao, H.-D., Kao, S.-J., Zhai, W.-D., Zang, K.-P., Zheng, N., Xu, X.-M., Huo, C., and
12 Wang, J.-Y.: Effects of stratification, organic matter remineralization and bathymetry
13 on summertime oxygen distribution in the Bohai Sea, China, *Cont. Shelf Res.*, 134,
14 15-25, doi:10.1016/j.csr.2016.12.004, 2017.

15 Zhu, C., Wagner, T., Pan, J.-M., and Pancost, R. D.: Multiple sources and extensive
16 degradation of terrestrial sedimentary organic matter across an energetic, wide
17 continental shelf, *Geochem. Geophys. Geosyst.*, 12, Q08011,
18 doi:10.1029/2011GC003506, 2011a.

19 Zhu, Z.-Y., Zhang, J., Wu, Y., Zhang, Y.-Y., Lin, J., and Liu, S.-M.: Hypoxia off the
20 Changjiang (Yangtze River) Estuary: oxygen depletion and organic matter
21 decomposition, *Mar. Chem.*, 125, 108-116, doi:10.1016/j.marchem.2011.03.005,
22 2011b.

23 Zimmerman, A. R. and Canuel, E. A.: A geochemical record of eutrophication and
24 anoxia in Chesapeake Bay sediments: anthropogenic influence on organic matter
25 composition, *Mar. Chem.*, 69, 117-137, doi:10.1016/S0304-4203(99)00100-0, 2000.

26 Zong, Y., Lloyd, J., Leng, M., Yim, W.-S., and Huang, G.: Reconstruction of Holocene
27 monsoon history from the Pearl River Estuary, southern China, using diatoms and
28 carbon isotope ratios, *Holocene*, 16, 251-263, doi:10.1191/0959683606hl911rp,
29 2006.

30
31
32
33

1 **Table 1.** Summary of end-member values and their uncertainties adopted in the three
 2 end-member mixing model.

Water Mass	$\theta(^{\circ}\text{C})$	Salinity	DIC ($\mu\text{mol kg}^{-1}$)	$\delta^{13}\text{C}_{\text{DIC}}$ (‰)	Ca^{2+} ($\mu\text{mol kg}^{-1}$)
Plume	30.6 ± 1.0	10.8	$1670 \pm 50^{\text{a}}$	$-7.0 \pm 0.8^{\text{b}}$	$3670 \pm 16^{\text{c}}$
Surface	31.0 ± 1.0	33.7 ± 0.2	1917 ± 3	0.6 ± 0.2	$9776 \pm 132^{\text{c}}$
Subsurface	21.8 ± 1.0	34.6 ± 0.1	2023 ± 6	0.1 ± 0.1	10053

3 ^a In order to derive a proper plume end-member value, we took advantage of 3 years of surface
 4 dataset from summer cruises (see Sect. 4.1). For DIC, the data is from cruises during August
 5 2012, July 2014 and July 2015.

6 ^b See details in Sect. 4.1.

7 ^c The Ca^{2+} values of the plume and surface seawater end-member are derived from a
 8 conservative mixing calculation (Ca^{2+} vs. S) based on 3 years of surface data during the summer
 9 (August 2012, July 2014 and July 2015).

10
 11
 12
 13
 14
 15
 16
 17
 18
 19
 20
 21
 22
 23
 24
 25
 26
 27
 28
 29
 30

1 **Table 2.** Comparison of $\delta^{13}\text{C}$ values in surface sediments within the hypoxic zone^a between
 2 the PRE and CJE.

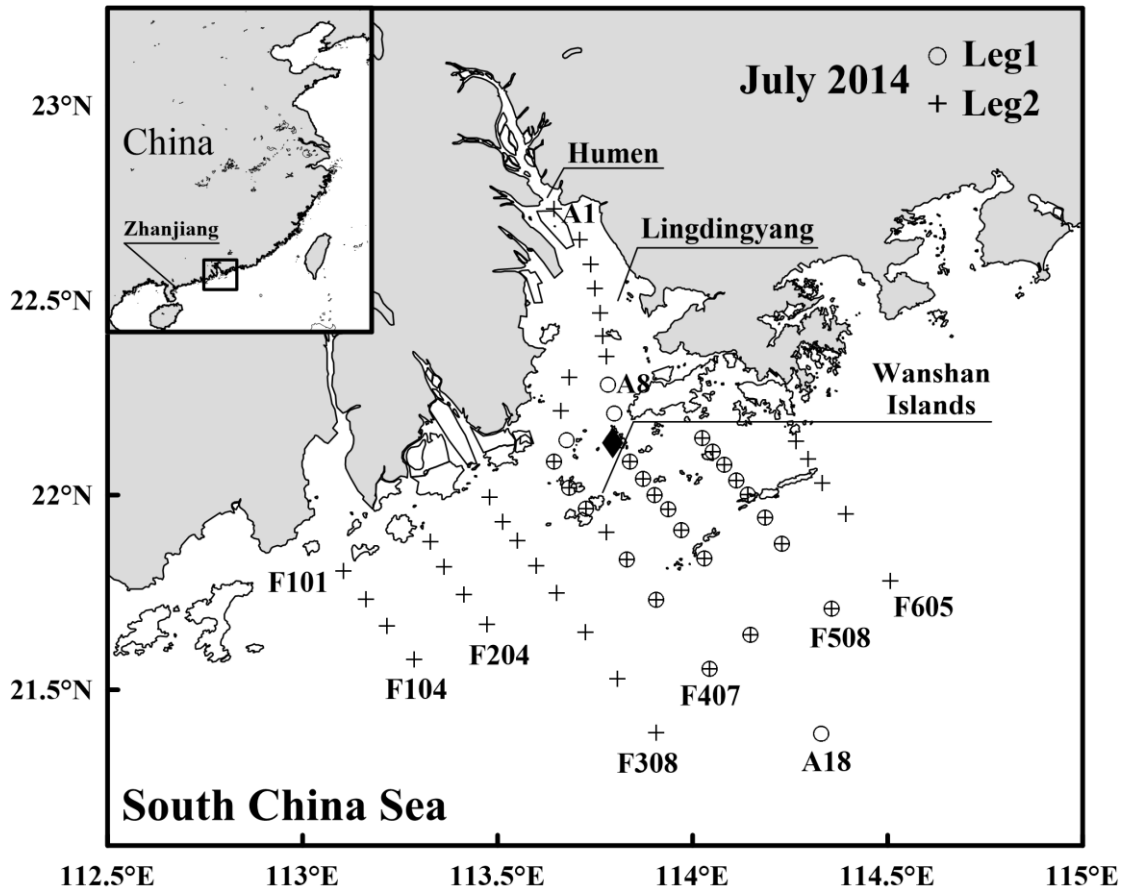
$\delta^{13}\text{C}$ (‰)	Mean \pm SD	Stations involved	References
<u>Pearl River Estuary</u>			
-23.4 ~ -22.1	-22.9 \pm 0.5	A4, A5, C1-C4, D1	Hu et al. 2006
-23.2 ~ -22.3	-22.7 \pm 0.5	28, 29, 30	Zong et al. 2006
-23.6 ~ -21.5	-22.5 \pm 1.1	E8-1, E7A, S7-1, S7-2	He et al. 2010a
- ^b	-23.1 \pm 0.6	Clustering groups G6 and G7	Yu et al. 2010
Average	-22.8 \pm 0.6		
<u>Changjiang Estuary</u>			
-22.9 ~ -20.9	-21.8 \pm 0.6	- ^c	Tan et al. 1991
-22.4 ~ -19.9	-21.2 \pm 1.0	32, 37, 38, 42, 48, 49, 54, 56, 64	Kao et al. 2003
-22.7 ~ -20.8	-22.0 \pm 0.8	H1-12, H2-10, H2-11, S1-2, S2-4	Xing et al. 2011
-23.5 ~ -20.4	-22.6 \pm 1.0	3, 12, 13, 20-25	Yao et al. 2014
Average	-21.9 \pm 1.0		

3 ^aIn the PRE, the data is from similar sites to our present study, which is in the northeast (Leg 1)
 4 and southwest (Leg 2) of the Wanshan Islands. While in the CJE, the hypoxic zone is located
 5 around 30.0 °N–32.0 °N, 122.7 °E–123.2 °E, which is frequently reported in previous studies
 6 (Li et al., 2002; Zhu et al., 2011b; Wang et al., 2016).

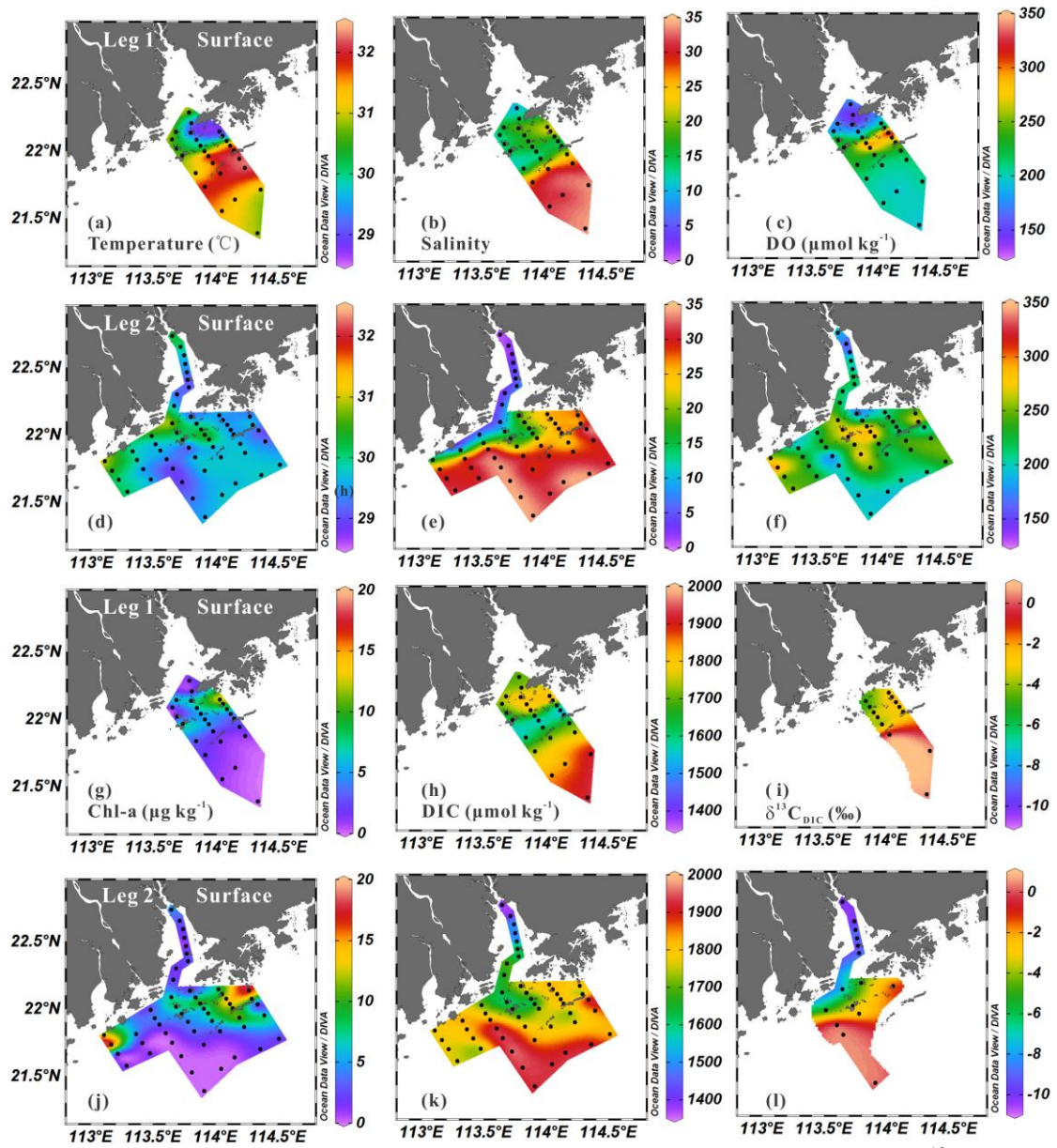
7 ^bThe authors provide an average value of clustering groups instead of individual data from each
 8 site.

9 ^cIn Fig. 7 of Tan et al. (1991), the sampling sites are shown without numbers.

10
 11
 12
 13
 14
 15
 16
 17
 18
 19

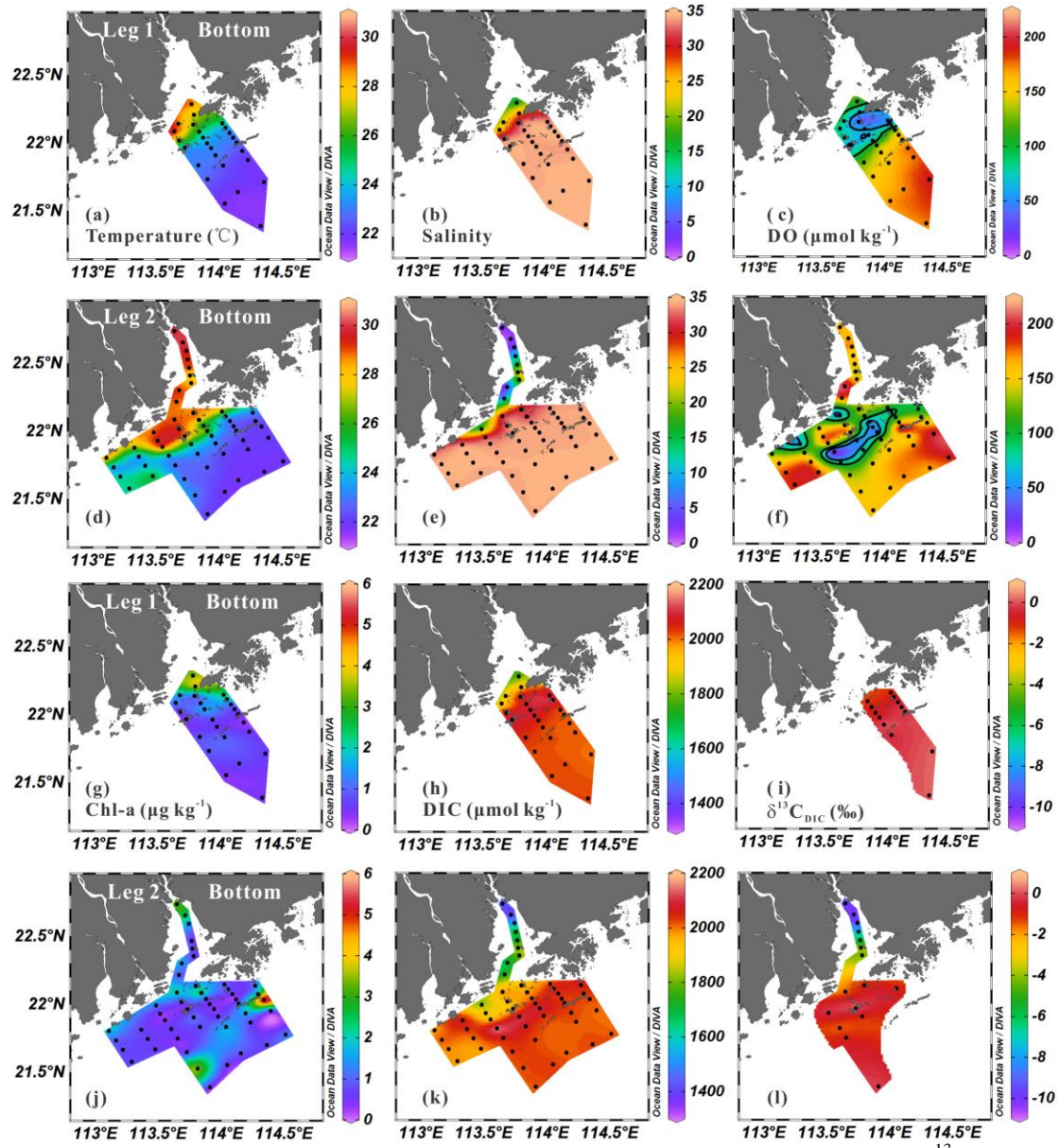


1
 2 **Figure 1.** Map of the Pearl River Estuary and adjacent coastal waters. The open circles denote
 3 Leg 1 stations visited on 13–16 July 2014, and the crosses represent Leg 2 stations visited on
 4 19–27 July 2014. Note that the filled diamond is the location of Station A10.
 5



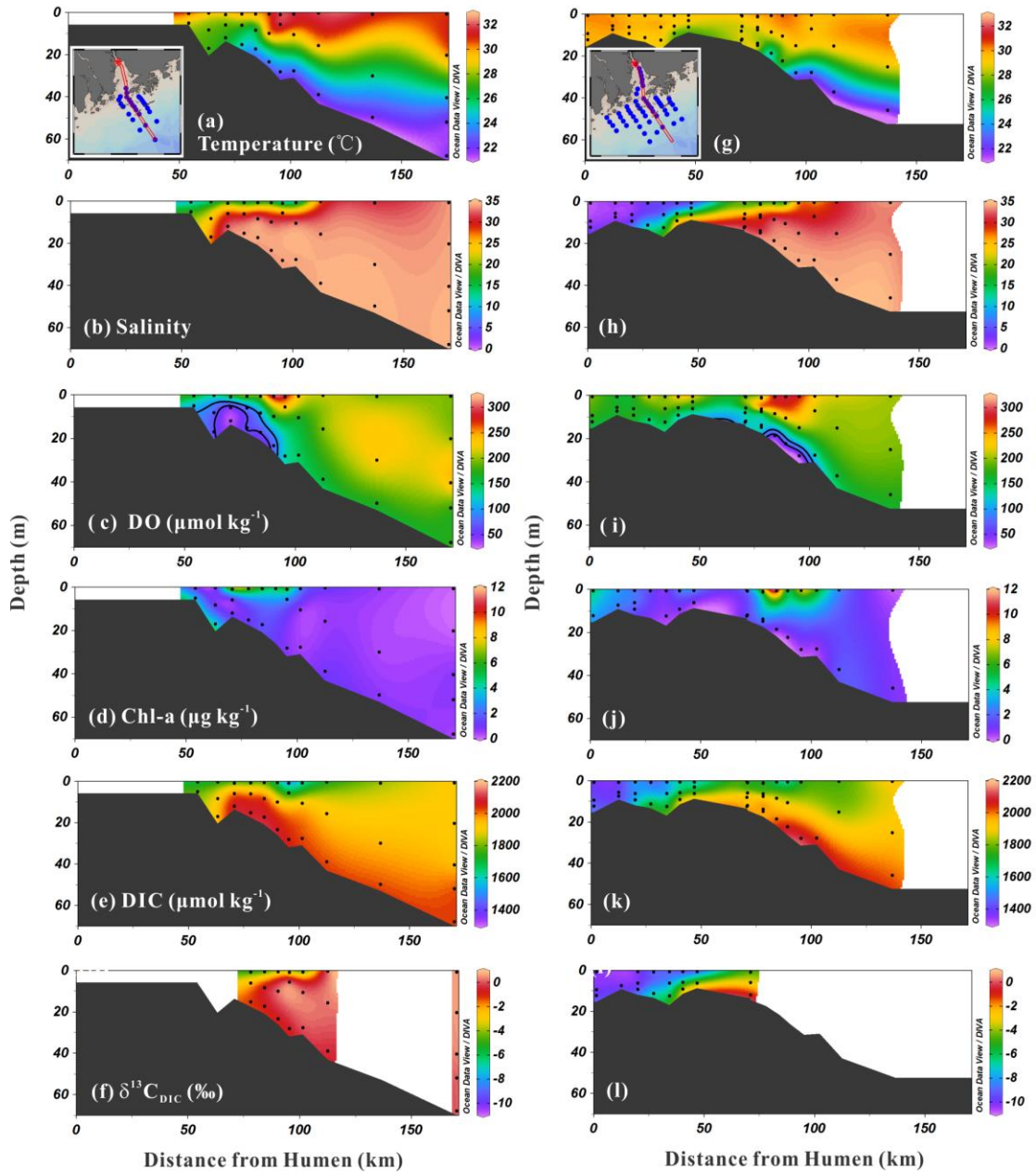
1
2 **Figure 2.** Surface water distribution of temperature, salinity, DO, Chl-a, DIC and δ¹³C_{DIC}
3 during Leg 1 (a–c, g–i) and Leg 2 (d–f, j–l).

4
5
6
7
8



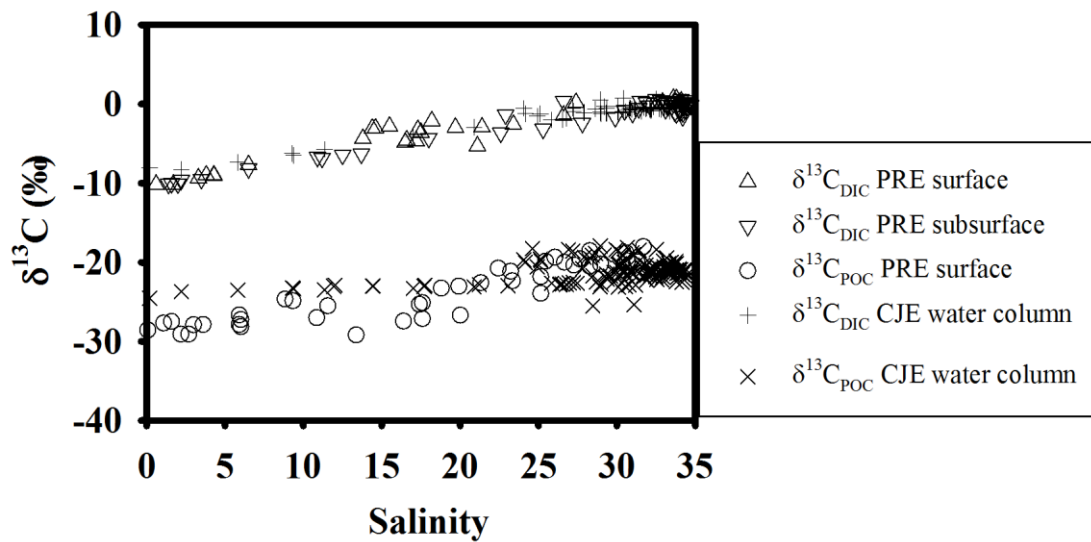
1
 2 **Figure 3.** Bottom water distribution of temperature, salinity, DO, Chl-a, DIC and $\delta^{13}\text{C}_{\text{DIC}}$
 3 during Leg 1 (a–c, g–i) and Leg 2 (d–f, j–l). Note that the black lines in (c) and (f) indicate DO
 4 contours of 63 μM and 95 μM .

5
 6
 7
 8
 9
 10
 11
 12
 13



1 Distance from Humen (km) Distance from Humen (km)
 2 **Figure 4.** Profiles of temperature, salinity, DO, Chl-a, DIC and $\delta^{13}\text{C}_{\text{DIC}}$ along Transect A
 3 during Leg 1 (a–f) and Leg 2 (g–l). Note that the black lines in (c) and (i) indicate DO contours
 4 of 63 μM and 95 μM .

5
 6

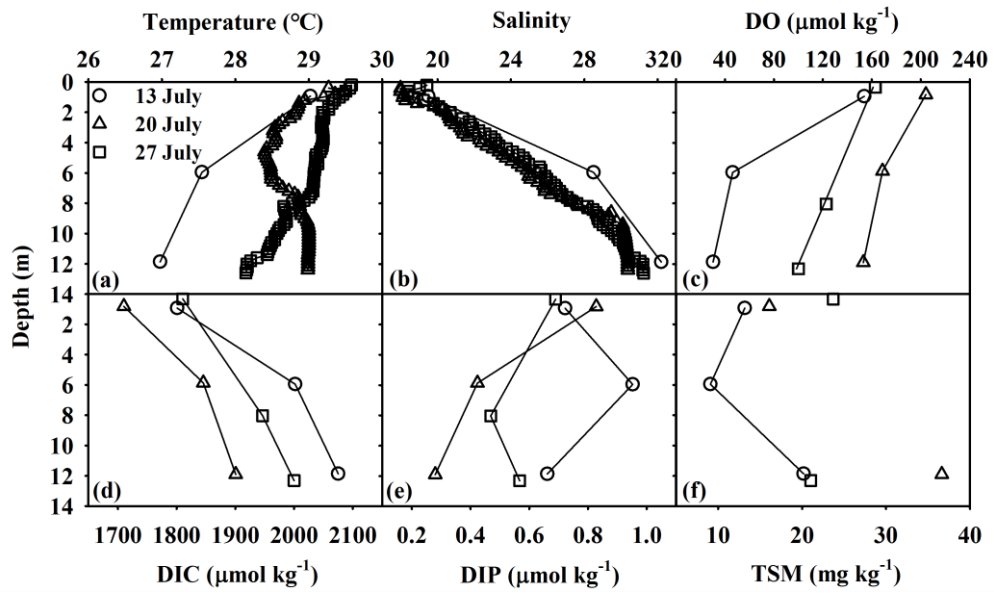


1

2 **Figure 5.** Distribution of $\delta^{13}\text{C}_{\text{DIC}}$ and $\delta^{13}\text{C}_{\text{POC}}$ with respect to salinity in the PRE. The up-facing
 3 and down-facing triangles denote surface and subsurface $\delta^{13}\text{C}_{\text{DIC}}$ data, respectively, from July
 4 2014, while the open circles represent $\delta^{13}\text{C}_{\text{POC}}$ values in surface water from July 2015.
 5 Additionally, the plus signs and crosses show the $\delta^{13}\text{C}_{\text{DIC}}$ and $\delta^{13}\text{C}_{\text{POC}}$ data, respectively, from
 6 the **Changjiang Estuary (CJE)** in Wang et al. (2016).

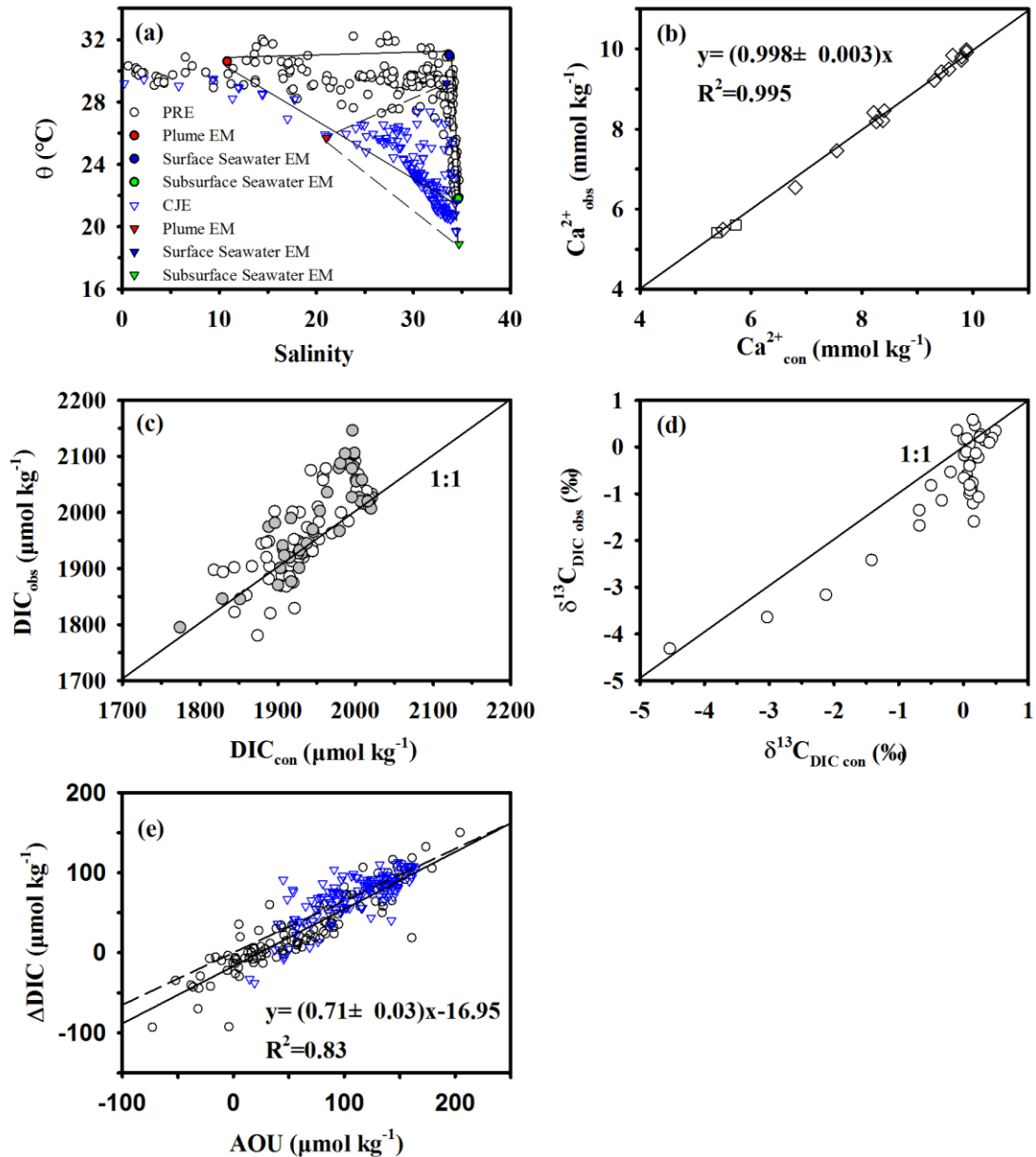
7

1



2

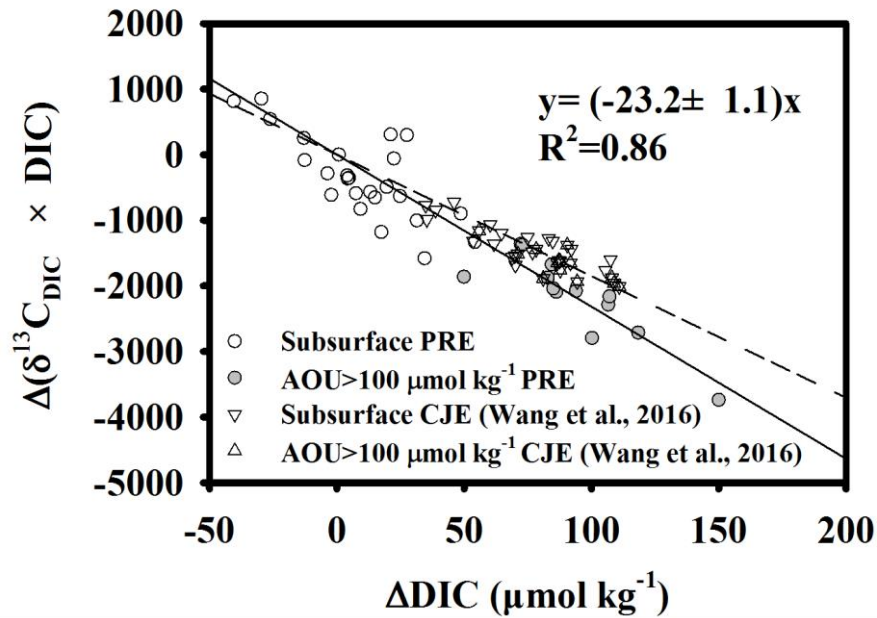
3 **Figure 6.** Profiles of (a) temperature, (b) salinity, (c) DO, (d) DIC, (e) DIP, (f) TSM and their
4 evolution during repeated sampling at Station A10.



1
2 **Figure 7.** (a) Potential temperature (θ) ($^{\circ}\text{C}$) vs. salinity in the PRE and adjacent coastal waters
3 (open circles) based on data collected during the July 2014 cruise. The three end-members are
4 shown as different coloured symbols. The blue triangles represent data collected during the
5 August 2011 cruise in the **Changjiang Estuary (CJE)** (Wang et al., 2016); (b) Correlation
6 between the field-observed Ca^{2+} ($\text{Ca}^{2+}_{\text{obs}}$) and **conservative** Ca^{2+} ($\text{Ca}^{2+}_{\text{con}}$). The straight line
7 denotes a linear regression line of both surface (square) and subsurface (diamond) data; (c), (d)
8 Relationship between observed and **conservative** DIC and $\delta^{13}\text{C}_{\text{DIC}}$ values. The straight line
9 represents a 1:1 reference line. Note that the grey dots in Fig. 7c identify data also in Fig. 7d;
10 and (e) Correlation of ΔDIC vs. AOU for all subsurface water data. ΔDIC is the difference
11 between the field-observed and **conservative** DIC concentrations. Also shown is the data from

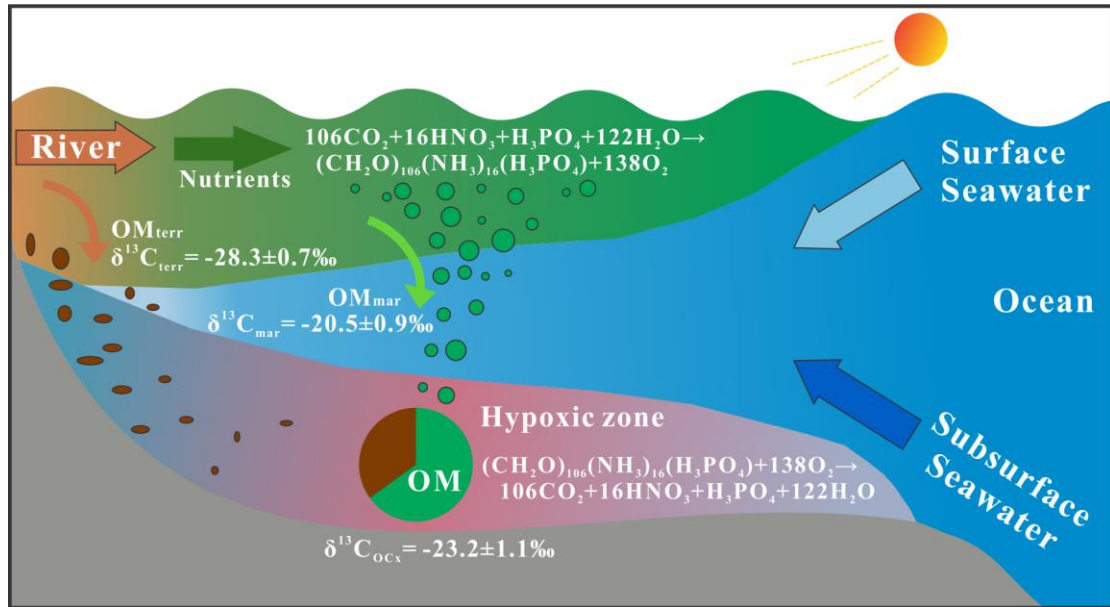
1 Wang et al. (2016). The straight and dashed lines indicate linear regressions of data from the
2 PRE and CJE, respectively.

3
4



5
6 **Figure 8.** $\Delta(\delta^{13}\text{C}_{\text{DIC}} \times \text{DIC})$ vs. ΔDIC in the PRE. Samples were collected from subsurface
7 water (> 5 m). The grey circles represent samples with $\text{AOU} > 100 \mu\text{mol kg}^{-1}$. Δ is the
8 difference between the field-observed and conservative values. Also shown is data from the
9 Changjiang Estuary (CJE) reported by Wang et al. (2016). The straight and dashed lines
10 indicate linear regression lines of data from the PRE and CJE, respectively.

11



1

2 **Figure 9.** A conceptual diagram illustrating the partitioning of oxygen-consuming organic
 3 matter (OC_{mar} vs. OC_{terr}) within the hypoxic zone in the lower PRE and the adjacent coastal
 4 area. See Sect. 5 for explanations.

5